STUDY TO REPLACE THE POWER SUPPLY OF A VALVE GUITAR AMPLIFIER WITH A SWITCH-MODE POWER SUPPLY

by

Gert Bleeker Kotze

Submitted in partial fulfilment of the requirements for the degree

Master of Engineering (Electronic Engineering)

in the

Department of Electrical, Electronic and Computer Engineering

Faculty of Engineering, Built Environment and Information Technology

UNIVERSITY OF PRETORIA

March 2019

SUMMARY

STUDY TO REPLACE THE POWER SUPPLY OF A VALVE GUITAR AMPLIFIER WITH A SWITCH-MODE POWER SUPPLY

by

Gert Bleeker Kotze

Supervisor(s):	Prof. W. P. du Plessis
Department:	Electrical, Electronic and Computer Engineering
University:	University of Pretoria
Degree:	Master of Engineering (Electronic Engineering)
Keywords:	Valve guitar amplifier, switch-mode power supply, non-linear power supply, and power amplifier.

This study investigates the possibility of replacing the existing unregulated power supply using valve rectifiers in a valve guitar amplifier with a switch-mode power supply to reduce the weight and size of the amplifier. Unregulated power supplies using valve rectifiers have high output voltages which tend to sag when the amplifier is driven into saturation. Research was conducted to identify a switch-mode power supply topology capable of reproducing the required response. This switch-mode power supply had to produce high output voltages with a non-linear output response, whilst maintaining control over the output voltage and current. Emulating an unregulated power supply using valve rectifiers in a valve amplifier with a switch-mode power supply by introducing non-linearities was challenging because these non-linear power supplies tend to have rather poor output regulation. Furthermore, the switch-mode power supply still had to be stable and predictable under varying load conditions. Feedback control was used to ensure that the error between the actual output response and the desired response was kept within a reasonable range to obtain a stable and regulated output response. An important outcome was that the switch-mode power supply should not introduce any switching noise on the output of the amplifier within the human audible range. The switch-mode power supply was integrated into a valve amplifier. Side-by-side tests were conducted on the valve amplifier that was

powered in turn by the unregulated and switch-mode power supplies. It can be concluded that it is indeed possible to replace the unregulated power supply using valve rectifiers in a valve amplifier with a non-linear switch-mode power supply, without affecting the dynamic response of the amplifier whilst being played.

LIST OF ABBREVIATIONS

AC	alternating current
DC	direct current
EMI	electromagnetic interference
ESR	equivalent series resistance
MOSFET	metal-oxide-semiconductor field-effect transistor
PCB	printed circuit board
PSRR	power supply rejection ratio
PWM	pulse width modulation
RMS	root-mean-square
THD	total harmonic distortion

TABLE OF CONTENTS

CHAPTER 1 INTRODUCTION

1.1 PROBLEM STATEMENT

The need to frequently travel long distances with bulky and heavy musical equipment poses a few challenges since weight and size restrictions are often imposed on luggage. When the first guitar amplifiers were designed, they were not necessarily designed to be transported over long distances, hence the bulky equipment. Modern valve guitar amplifiers are still built using the same design as that of the original amplifiers. Consequently, these amplifiers were never optimised in terms of size and weight. The unregulated power supply using valve rectifiers is one of the largest and heaviest sub-components in a valve amplifier and could be replaced with a smaller, lighter and more efficient switch-mode power supply [1–3]. The unregulated power supply using valve rectifiers is heavy and bulky since it is constructed from a large AC mains transformer with a soft iron core that needs to be air cooled as well as rectifier tubes that need to be mounted securely to dampen vibrations to these tubes which could damage them. One concern with replacing the unregulated power supply using valve rectifiers with a switch-mode power supply is that the dynamic response and the sound of the amplifier would be affected [1, 3]. Commercially available switch-mode power supplies have a different transient and frequency response than that of an unregulated power supply because the former is designed to have a stable, linear and regulated output response. The unregulated power supplies using valve rectifiers in valve amplifiers are non-linear and the output voltage tends to sag at high load conditions seeing that the power transformer and vacuum tube diodes saturate when the current draw is high [1, 4].

Thus, a switch-mode power supply had to be developed to produce the same non-linear output response with output saturation as that of an unregulated power supply while maintaining a stable and controlled output voltage. Research was conducted to understand how a switch-mode power supply could be

designed to produce a non-linear output response with output saturation because all switch-mode power supplies are currently designed to have a stable and linear output.

1.2 CONTEXT OF THE PROBLEM

The guitar became popular during the 1950s, and as music concerts grew, the guitar had to compete with louder instruments and crowd noise [4,5]. This led to the development of an electric guitar and amplifier powered by an unregulated power supply [5]. At the time, the only method of amplifying signals was by using valves as the main amplification device in amplifiers [4, 5]. The valves, however, introduced non-linearities that led to signal distortion, but as time passed, this became a favourable sound-effect with musicians as they can exploit these non-linearities to control the sound of the instrument [4,5]. Because of this, musicians could develop a characteristic sound unique to them. Amplifiers, using valves as the amplification device, are often described as having a rich or warm sound, whilst modern transistor-based amplifiers are lacking this unique quality. This is also the reason why valve amplifiers are still in such high demand with musicians and music enthusiasts [4].

The power supplies of traditional amplifiers were designed to be as cost-effective as possible, resulting in undersized power supply transformers being used [1,4]. The valve rectifier introduces additional resistance into the circuit, as opposed to modern diodes which, in turn, reduces the current flow and contributes to power supply sag. Power supply sag is the output voltage drop of the power supply as more and more current is being drawn. This increases the amount of ripple on the output of the power supply because it is not regulating the output voltage and cannot keep up with the demand if the guitar is being played hard and the amplifier is thus driven hard [1]. The power supply sag will only occur when the amplifier is driven very hard, in other words, near its saturation point when chords and individual notes are struck forcefully [6–8]. It was then noted that the power supply sag, in combination with bias shift output, transformer saturation, and asymmetrical valve clipping produced a compression effect that was pleasing to the ear [1,9,10]. This combination of effects gives a valve amplifier its very unique sound and feel [9–12].

One of the advantages of unregulated power supplies in valve amplifiers is that they are simple to construct and maintain because they are manufactured with fewer, less complex components as opposed to a regulated linear or switch-mode power supply [6,7]. This ensures that the valve amplifier has good

reliability because it has fewer components that can fail, and the manufacturing time of the amplifier can be reduced seeing that the design is simple. These amplifiers are favoured by musicians because they seem to prefer the unique influence on the sound caused by power supply saturation [6,7,9].

A disadvantage of unregulated power supplies is that they require a large mains alternating current (AC) transformer to generate the required output voltages and are therefore heavy and bulky [3]. These power supplies also tend to operate at higher temperatures because they are fairly inefficient and produce too much heat that needs to be dissipated to avoid damage to the components [6,7]. As a result of the higher operating temperature of especially the mains AC transformer, it tends to overheat and fail when the amplifier is played for prolonged periods of time on high volume settings [6,7,12].

The mains AC transformer is normally wound to be used with a specific input voltage, but the mains AC supply voltages differ in some countries [6,7,12]. This means that the transformer in an unregulated power supply will need to be changed if musicians want to use the amplifier in a country with a different supply voltage. It also means that amplifier models must be manufactured to cater for the different mains input voltages across the world.

Another disadvantage of the unregulated power supply is that it introduces a hum on the output of the amplifier which interferes with the sound. Musicians differ in their opinion regarding whether a valve amplifier should hum or not. The argument for a hum is that it is a traditional sound associated with a valve amplifier, while the opposing opinion is that it creates too much interference.

According to research, it is possible to replace the unregulated power supply in a low power class A valve amplifier with a switch-mode power supply, without affecting the sound, when a constant peak amplitude sinusoidal wave is presented as the input signal [3]. The main contributing factor to this success is that the switching frequency of the switch-mode power supply was high enough not to influence the sound within the human audible range [3]. The effects of the power supply on the class A valve amplifier and how it influences the sound being produced were, however, not investigated.

It is thus clear that the unregulated power supplies which are traditionally used in valve amplifiers to supply power to the heaters and valve plates result in a heavy and bulky solution which is difficult to handle [6,7,9]. One solution to the problem is to implement a switched-mode power supply. This approach will deliver the same amount of power to the amplifier, but it will be lighter, smaller and more

efficient than an unregulated power supply [6,7]. If the switching frequency is higher than 20 kHz, the human ear will not be able to hear the switching noise and it will be outside the frequency response of the speaker [3].

To successfully replace the unregulated power supply in a valve guitar amplifier with a switch-mode power supply, will require that this supply has the same transient response as the unregulated power supply under similar load conditions. To accomplish this, the switch-mode power supply would have to be highly non-linear to introduce power supply saturation. This is, however, the exact opposite design to normal linear and stable switch-mode power supply designs [13–15]. Research had to be conducted on how to design a switch-mode power supply with a similar output saturation curve as an unregulated power supply, while still having control over the output voltage and current.

A fair amount of research exists on how to design a switch-mode power supply that is highly linear whilst having a closely regulated output voltage [13–15]. Little information is currently available on how to design a non-linear, but still stable, switch-mode power supply with a variable transient response. Research on how to design and build this power supply had to be conducted before it could be designed and tested so that the possible effects of the power supply on the valve amplifier could be investigated.

All the effects of the power supply on the response of valve amplifiers are not yet known and documented. These effects were critical in the research of a switch-mode power supply to ensure that it produces the same sound and distortion as a valve amplifier powered by an unregulated power supply. Therefore, research on these effects was conducted and used to determine the important transient response properties of the power supply that had the biggest influence on the dynamic response and distortion produced by valve amplifiers.

1.3   RESEARCH GOALS AND APPROACH

1.3.1   Research goals

A number of aspects had to be investigated to determine whether the unregulated power supply in a valve amplifier could be replaced with a switch-mode power supply with similar performance

characteristics without affecting the sound and distortion of the amplifier.

- The first aspect relates to how the output voltage and current of the power supply in a valve amplifier respond to a guitar input signal.

- The second aspect relates to how a switch-mode power supply could be designed to have a non-linear output with similar saturation characteristics as an unregulated power supply, whilst still maintaining control over the output voltage and current.

- The third aspect is the influence of a switch-mode power supply on a high output power class AB valve amplifier. By researching this, it would be determined whether the switch-mode power supply added extra noise to the sound produced by the amplifier and whether or not the switching noise fell within the human audible range. It would also be known whether the valve amplifier still produced the same sound and distortion when powered with a switch-mode power supply or not.

1.3.2   Approach

The research project was planned in the following phases.

- The transient response of the unregulated power supply was tested while it was connected to a valve amplifier under load.

- Once the effects of the power supply on the sound of the valve amplifier were known and the unregulated power supply characterised, a switch-mode power supply design was studied in-depth to determine the effect of each component in the circuit. The information gained from this phase was used to conduct further studies on non-linear switch-mode power supplies and on how to obtain stable output characteristics. This study also indicated how the transient response of a switch-mode power supply could be changed to obtain different output responses. Knowledge was obtained on how the switch-mode power supply could be made non-linear whilst still maintaining control over its output voltage and current. Emulating an unregulated power supply in a valve amplifier with a switch-mode power supply by introducing non-linearities could be

challenging because these non-linear power supplies tend to have rather poor output regulation, while the switch-mode power supply still has to be stable under varying load conditions.

- Once the study clarified which components had to be changed, the switch-mode power supply was designed and tested. The test results were compared to the measurements obtained from tests where the valve amplifier was powered by the unregulated power supply.

- The switch-mode power supply was then tested to ensure that it performed similarly to the unregulated power supply under full load and, where necessary, changes were made. The objective of this phase was a switch-mode power supply that has the same transient response and frequency response within the human audible range as the unregulated power supply tested in Phases one and two.

- The switch-mode power supply was integrated into a valve amplifier and side-by-side tests were conducted on the valve amplifier that was in turn powered by the unregulated and switch-mode power supplies. Once these results were known, a conclusion could be drawn on whether or not it was possible to replace the unregulated power supply in a valve amplifier with a non-linear switch-mode power supply without affecting the dynamic response of the amplifier whilst being played.

1.4   METHODOLOGY

A switch-mode power supply had to be constructed with the same transient and frequency response as that of an unregulated power supply. To accomplish this, research was conducted to identify different switch-mode power supply topologies capable of delivering high output voltages. The transient response of the unregulated power supply was analysed, while it was connected to a valve amplifier and under load. From this, the effect of the power supply on the dynamic response of the amplifier could be obtained. Once the different topologies for the switch-mode power supply were identified, and the effect of the power supply on the dynamic response was known, these topologies could be researched further to identify the exact function and contribution to the transient and frequency response of each component.

The information gained from this phase was used to conduct further research on non-linear switch-mode power supplies and on how to obtain stable output characteristics. Knowledge was obtained on how the switch-mode power supply could be made non-linear, whilst maintaining control over its output voltage and current. Emulating an unregulated linear power supply in a valve amplifier with a switch-mode power supply by introducing non-linearities, was challenging because non-linear power supplies tend to have rather poor output regulation. Furthermore, the switch-mode power supply still had to be stable and predictable under varying load conditions. Feedback control was used to ensure that the error between the actual output response and the desired response was kept to a minimum. This implied that the control would be closed-loop rather than open-loop since the output measurement is fed back to the controller to compensate for any discrepancies, and to obtain a stable and regulated output response. This knowledge gained was subsequently used to design a switch-mode power supply with a specific output impedance and the required transient and frequency responses.

The switch-mode power supply was integrated into a valve amplifier. Side-by-side tests were conducted on the amplifier that was powered in turn by the unregulated and switch-mode power supplies. Once these results were analysed, a conclusion was drawn whether it was indeed possible to replace the unregulated linear power supply in a valve amplifier with a non-linear switch-mode power supply, without affecting the dynamic response of the amplifier whilst it is being played.

1.5 HYPOTHESES

The following hypotheses were formulated for this research project.

- The power supply has an influence on the dynamic response of a valve amplifier. The amount of clipping in the power stage of the amplifier is dependent on the output voltage of the power supply. The output voltage and the output impedance will also have an influence on the characteristic curve of the vacuum tube and, therefore, on the sound of the amplifier. The power supply can thus be used to move the operating point on the characteristic curve of the vacuum tube.

- It is possible to recreate the power supply saturation response of an unregulated linear power supply with a carefully designed switch-mode power supply. This will be achieved mainly by modifying the feedback network to obtain a slower output response. The switch-mode power

supply controller can be replaced with a microcontroller to gain more control over the output voltage and, thus, the transient response. The output of the power supply can be made non-linear by modifying the feedback network and the controller. By doing this, it should be possible to build the required output transient response into the controller as well as into the feedback network.

- The transient response of the power supply will have a large effect on the amount of distortion produced by the amplifier. It will also influence the clipping point of the power stage because it is highly dependent on the output voltage of the power supply. When the switch-mode power supply has the same transient response as an unregulated power supply in a valve amplifier and if the switching noise can be eliminated, it should not have any additional effect on the amplifier.

- If the switching frequency of the switch-mode power supply is kept high enough, the switching noise should not influence the sound of the amplifier because the frequency of the noise will be above the human audible range and outside the frequency response of the speaker. This should deliver a clean audio signal on the output of the power stage with minimal switching noise.

1.6   RESEARCH CONTRIBUTION

From this research, knowledge was obtained on how the transient response of a switch-mode power supply could be changed to introduce non-linearities to effectively make it an unregulated, but still stable and predictable, power supply. The effect of the power supply on a valve guitar amplifier was also deduced. It was determined that an unregulated linear power supply can be replaced with a more efficient and compact switch-mode power supply without affecting the dynamic response of an amplifier. This will enable designers of valve amplifiers to design a product that is smaller in size and lighter in weight, and in doing so, making it easier to move and transport the amplifier. The unregulated linear power supply in existing valve amplifiers can also be replaced with a switch-mode power supply to reduce the weight of the amplifier.

This research on the effects of a power supply on valve amplifiers can be used by valve amplifier designers to change the response of an amplifier to suit individual musicians' needs and to generate a unique guitar sound applicable to different music genres. It can potentially be used by designers

who wish to develop solid-state replacements for valves since the difference in vacuum tube responses, depending on the transient response of the power supply, is better understood after this research. This also opens the opportunity to develop compact valve amplifiers that can be built into pedals. This research has several varying application possibilities since there are many products that can benefit from it.

1.7   EXPECTED OUTCOMES

- The power supply has an influence on the dynamic response of a valve amplifier. The amount of clipping in the power stage of the amplifier is dependent on the output voltage of the power supply [4, 6, 7, 16]. The output voltage and the output impedance of the power supply also have an influence on the characteristic curve of the vacuum tube and, therefore, on the sound of the amplifier [6, 7, 10, 16]. The power supply could, therefore, be used to modify or change the characteristic curves of the vacuum tubes.

- An expected outcome was that it is possible to recreate the power supply saturation response of an unregulated linear power supply with a carefully designed switch-mode power supply. This could mainly be done by modifying the feedback network of the power supply and by using a microcontroller to control the outputs of the power supply [13, 15, 17]. The output can be made non-linear by modifying the feedback network, output filters and controller [13, 14, 17]. In doing this, it would be possible to build the required output transient response into the feedback network, output filter and controller [13–15, 17].

- Another expected outcome was that the transient response of the power supply would have a large effect on the amount of distortion of the amplifier [16]. It would also influence the power stage clipping point of the amplifier since the latter is highly dependent on the output voltage of the power supply [6, 7, 16]. With the switch-mode power supply having the same transient response as that of an unregulated power supply in a valve amplifier, and if the switching noise could be eliminated, it was expected that it should not have any additional effects on the amplifier.

CHAPTER 2   LITERATURE STUDY

2.1   CHAPTER OBJECTIVES

This chapter will discuss the different types of power supplies that can be used to power valve amplifiers. The different types of unregulated, linear and switch-mode power supplies will also be discussed below.

2.2   AMPLIFIER POWER SUPPLIES

Several different types of power supplies can be used to power a valve guitar amplifier, such as an unregulated power supply, a regulated linear power supply and a regulated switch-mode power supply [6, 7]. The unregulated power supply using valve rectifiers is, however, the most commonly used in amplifier designs because it is simple and cheap to manufacture and musicians like the clipping caused when the power supply saturates [6, 7]. These unregulated power supplies have few parts and the reliability is good since there are fewer components in the power supply that can fail or cause a problem [7]. A major drawback of the unregulated and regulated linear power supplies is that both make use of a large and heavy transformer with several different taps on the windings to generate the required output rail voltages [6, 7]. They also need to cater for the different mains supply voltages used across the world by adding, even more, taps on the primary side of the transformer and, in doing so, further increasing its design complexity. The current that flows through the primary windings will increase if the supply voltage is lower, thus heavier gauge wire will be required. The higher current flow will generate more heat in the transformer which needs to be dissipated.

The regulated linear power supply makes use of additional complex circuitry to limit the output current

of the power supply and to regulate or keep the output voltage at a constant level [7]. This, in turn, introduces extra components into the power supply design that can cause possible failures; more heat is also generated because the regulators produce substantial heat while regulating the output voltage. These complexities necessitate a skilled designer to design a stable, regulated linear power supply with care [6, 7]. The introduction of new components and a complex design will increase costs while adding little value since the size, efficiency and weight of the complete amplifier will not change and the performance of the amplifier will not increase noticeably. The main advantages of a regulated linear power supply are that it has a low output voltage ripple and the power supply rejection ratio (PSRR) restraint, which unregulated and switch-mode power supplies have, can be relaxed if the output voltage ripple can be kept steady with sudden current demands. By doing this the noise on the output rails of the power supply has been significantly reduced [6, 7].

A switch-mode power supply is the least commonly used type of power supply in valve guitar amplifiers seeing that they are complex to design, build and test [6, 7]. This type of power supply has multiple components and complex circuitry that could cause more failures and problems than an unregulated power supply that has fewer components [7]. The switch-mode power supply, however, has a lot of advantages over an unregulated power supply, such as low output ripple, higher efficiency, they can function over a variety of input voltages and can, thus, be used all over the world because the different mains supply voltages will not influence its operation [3, 7, 17]. The biggest advantage of a switch-mode power supply over an unregulated or regulated linear power supply is that they use a small transformer that reduces weight and size [3, 7, 17]. This will result in a more compact and lightweight amplifier unit that can be transported more easily.

Different power supply types and power supply design considerations for valve amplifiers are now discussed.

2.2.1   Existing linear and unregulated power supplies

Several different techniques and component choices are made during the design of a power supply leading to several different power supply designs, each with their own unique transient response to changes in current draw [6, 7]. The two distinct differences in unregulated power supply designs are the use of (i) silicon rectifiers or (ii) vacuum tube rectifiers for the primary rectifying device [6, 7, 11, 12, 16].

The characteristic response of a silicone rectifier differs from that of a vacuum tube rectifier [6, 7, 11, 12, 16]. This will create a different transient response in the output of the power supply depending on the use of a silicone or vacuum tube rectifier and the amount of current being drawn. The biggest difference between a silicone rectifier and a vacuum tube rectifier can be seen under continuous high load conditions because the vacuum tube rectifier has a lower continuous forward current compared to that of a silicone rectifier [2, 6, 7, 12]. As a result of this, the amplifier will have a different sound when it is played hard or if a few chords are struck forcefully by the musician. These actions will draw more current from the power supply and will place a higher load on the transformer and rectifier, thus resulting in power supply sag [2, 6–8].

The transformers that are used in unregulated power supplies for valve amplifiers are built as cheaply as possible to ensure that the amplifier is cost effective and price competitive in the market [2, 6, 7, 12]. This is done by lowering the safety factors of the design but, however, leads to transformers that are wound with thinner gauge copper wire and transformer cores made of iron alloys [2, 6, 7, 12]. A result of this is that the transformer will operate at higher temperatures because the transformer windings start to heat up from the higher current flowing through them [2, 6, 7, 12]. The transformer can then prematurely fail if the heat build-up is not properly managed.

If the transformer is poorly constructed, it could also influence the sound produced by the amplifier because the output voltages will start to sag prematurely if the current drawn from the power supply increases [2, 6, 7, 12]. Power supply transformer sag is caused by heat build-up in the transformer as well as transformer core saturation where the transformer core is magnetised into saturation and cannot be magnetised any further [7, 17]. This leads to a transformer that is highly non-linear and has unpredictable output voltages [7, 17].

The unregulated power supply has, however, been known to give valve amplifiers a unique response when the output voltage starts to drop as a result of power supply saturation [2, 6, 7, 12]. This drop in the output voltage causes clipping in the power stage of the amplifier which, in turn, causes distortion of the audio signal [2–5]. What makes this a unique phenomenon is that the clipping only occurs when the guitar is played forcefully and that the amount of clipping varies as the output voltage of the power supply varies [2, 6, 7, 12]. When the output voltage recovers sufficiently, the amount of clipping is reduced and normal operation continues [2, 6, 7, 12].

2.2.2 Linear switch-mode power supplies

Switch-mode power supplies are normally developed to replace bulky linear power supplies with a supply that is compact, lightweight and more efficient and it also produces less heat [3, 17]. Modern switch-mode power supplies have power factor correction built in, ensuring higher efficiency [3, 17]. This is done by adding a power factor correction circuit enabling the non-linear switch-mode power supply to seem like a linear load to the electrical network that it is connected to [17]. Power factor correction circuits minimise the reactive power drawn from the mains power supply, thus lowering the apparent power draw to levels that are closer to the actual power draw [18]. This results in less heat being generated in the wiring making the power supply more efficient as the voltage and current waveforms are in phase with each other [13, 18].

Switch-mode power supplies usually make use of negative feedback networks to regulate the output voltage as closely as possible to the desired set-point and to linearise the power supply system [13, 19]. This results in a power supply that produces a regulated output voltage with little sag on the outputs when the current draw is increased, with the only condition being that the total amount of power drawn is not exceeded [13, 19]. The feedback network is designed to ensure that the power supply is stable for a certain frequency range in which it will normally operate to ensure that the output voltage does not start to oscillate [13, 19] . The feedback network is thus used to add poles and/or zeros to the system to ensure stability [13, 19].

The feedback network in a switch-mode power supply is used to change or modify the output to produce different output responses [13]. This is a useful property because it can be used to change the transient response which can then be used to reproduce the transient response of an unregulated power supply with vacuum tube rectifiers. It will, in turn, create a poorly regulated power supply with a variable transient response when compared to a standard switch-mode power supply, while still having control over the output voltage.

2.2.3 Valve amplifier switch-mode power supply design

Switch-mode power supplies allow safety features such as over voltage, over current and surge protection to be incorporated into the design [13, 19]. The power supply could have a safety function to detect

failed tubes as the current drawn will be lower than normal and can then readjust its output voltages accordingly to keep the supply rails within the recommended operating conditions. Measurements of the voltage and current drawn at the outputs ensure that the power supply is operated within its designed limits, and to ensure that it will not prematurely fail because of overloading or excessive heat build-up [13, 19].

The amount of electromagnetic interference (EMI) and switching noise generated by the switch-mode power supply can be significantly reduced by implementing electromagnetic filters in line with the output rails [20–22]. This reduces the amount of conducted EMI from the power supply. The switch-mode power supply module is shielded from the rest of the amplifier to reduce the amount of radiated EMI [20–22]. By using these two techniques it is possible to eliminate most of the interference that a switch-mode power supply normally generates. This also reduces the amount of hum that can be heard from the amplifier when it is not being played.

2.2.4   Switch-mode power supply topologies

Several different topologies are being used in switch-mode power supply designs. Each topology has its own benefits and shortcomings which should be considered before one can be selected for a design. The switch-mode power supply topologies are categorised as isolated and non-isolated.

The isolated topologies provide isolation from the mains electricity supply by using a transformer and opto-isolator to isolate the secondary side of the power supply from the primary side [23]. This is an important aspect to consider in consumer electronics with exposed conductive parts that could cause an electrical shock hazard for the user. By isolating the secondary side of the power supply from the primary side, a new zero volt reference point is created that is connected to the safety earth of the unit [23]. This eliminates high voltage floating ground points that can cause an electric shock. Isolation also reduces the coupling of transients from the primary side of the power supply and also removes ground loops in the power supply. The different types of isolated topologies commonly used are the flyback, forward, half bridge and full bridge [23, 24]. These topologies are more complex than non-isolated topologies because the feedback network needs to be isolated and the transformer needs to be switched at high voltages and frequencies [23, 24]. By doing this, it reduces switching losses and

since the change in magnetic field is rapid, the transformer size can be decreased while maintaining the same power delivery as that of a larger transformer being switched at a lower frequency [19, 23].

The non-isolated topologies usually have a smaller footprint than the isolated topologies since they do not require a transformer to provide isolation. The non-isolated topologies also need fewer components and are therefore more cost-effective than isolated topologies. One shortfall of the non-isolated topology is that the output is always referenced to the main supply voltage and can, therefore, have high voltages on conductive parts because the zero volt terminal of the output cannot be connected to the safety earth [23, 24]. The different types of non-isolated topologies are the buck (step-down), boost (step-up) and buck-boost (step-up and step-down) converters [23, 24]. These converters are also known as direct current (DC) to DC converters because they receive a DC input voltage and generate a DC output voltage.

2.3   ISOLATED SWITCH-MODE TOPOLOGIES

The isolated topologies are discussed in this section to identify the benefits and shortfalls of each. A brief circuit description with critical waveforms is also presented for each of the topologies.

2.3.1   Flyback topology

The flyback topology, shown in Figure 2.1, is normally used in applications where the required output power ranges from 30 W up to 250 W [19, 23, 24]. The output power for this topology has to be stored in the core of the transformer as a magnetic field for part of a duty cycle [19, 23, 24]. This means that the cost and size of the core will be higher than that of other isolated topologies since a larger core is required to store the energy. This topology also requires a low primary inductance for the transformer because high peak currents are required to transfer the energy from the primary side of the transformer to the secondary side [19, 23, 24]. To accomplish this, the transformer is gapped so that most of the high peak energy can be stored in the transformer gap and, by doing this, transformer saturation will be avoided [19, 23, 24]. One drawback of this topology is that when the switching transistor or metal-oxide-semiconductor field-effect transistor (MOSFET) turns off, the output voltage is reflected on the primary side of the transformer. A turn off voltage spike is also present due to the transformer leaking inductance on the primary side [19, 23, 24]. Combining these effects, mean that
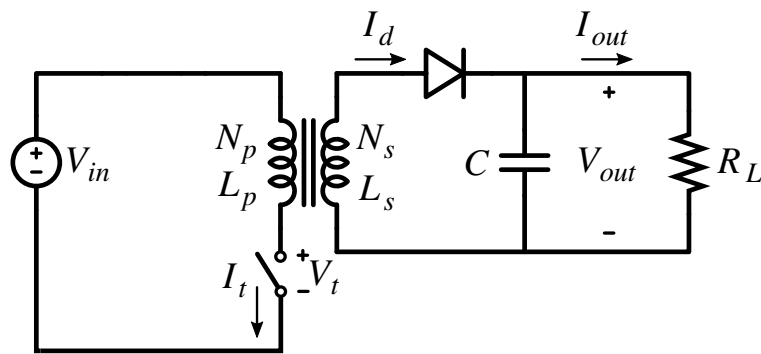
Figure 2.1. Flyback topology [19].

the switching transistor or MOSFET has to block double the supply voltage plus the leakage spike, implying that the primary switching device is subjected to high voltages, putting more strain on this device.

During the on cycle, the transformer acts like an inductor by storing energy in the transformer core and the output current is supplied by the output capacitor. The current flow through the primary winding and switch i_T, as well as the current flow through the secondary side diode, are shown in Figure 2.2. From this, it can be seen that the current flow through the primary winding increases linearly from its initial value to the peak input current I_{pk}. From Figure 2.2 it can also be seen that the voltage over the switch V_T is the sum of the input voltage and the product of the output voltage and turn ratio.

2.3.2 Forward topology

The forward topology, shown in Figure 2.3, has a continuous output current through the inductor i_L, meaning that the power supply output has a low output voltage ripple and also that a smaller output capacitor can be used as shown in Figure 2.4 [19, 23, 24]. The energy in this topology is directly transferred through the transformer instead of storing it during part of the duty cycle [19, 23, 24]. This type of converter, therefore, does not need a gapped transformer core and can have a high primary inductance [23]. Since almost no energy is stored in the core, except for the magnetisation energy, the transformer is smaller than that of a flyback converter. The stress on the primary switching device is lowered by using a clamp winding on the primary side of the transformer [19, 23, 24]. This winding conducts the leakage inductance voltage spike back to the supply and demagnetises or resets the transformer core at the end of each duty cycle [19, 23, 24]. However, the switching transistor or
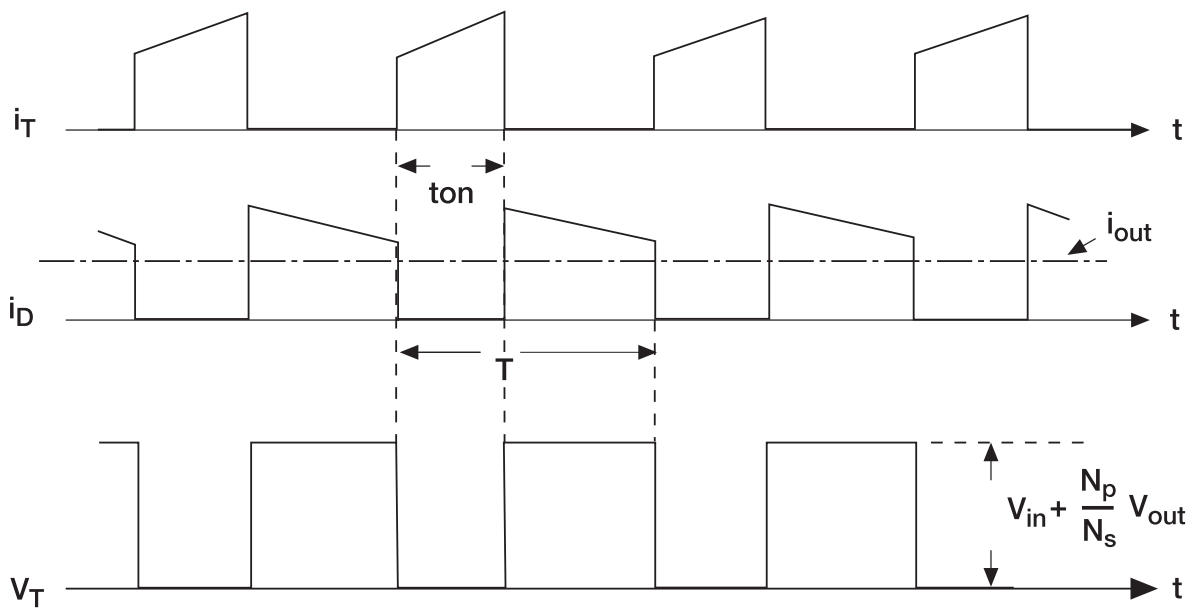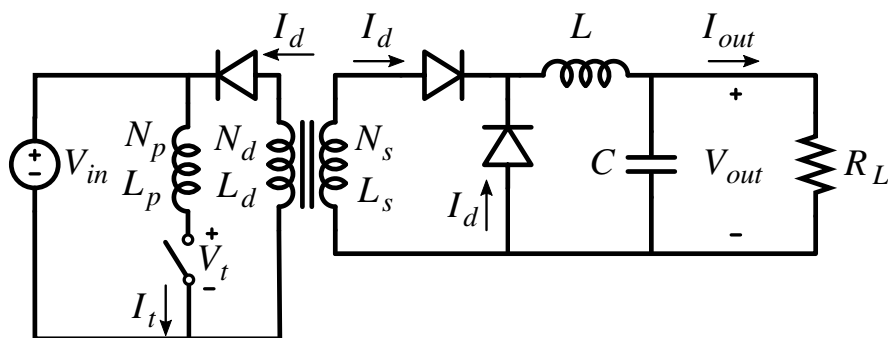
Figure 2.2. Flyback topology waveforms [19].

Figure 2.3. Forward topology [19].

MOSFET still has to withstand twice the input voltage, since the latter is reflected on the primary side of the transformer during demagnetisation.

When the switch is on, the magnetization current i_{mag} increases linearly from 0 to $\frac{V_{in}}{L_M}$, where L_M is the magnetizing inductance of the primary winding of the transformer as shown in Figure 2.4. The total current i_T flowing through the switch and primary windings of the transformer is the reflected output inductor current i_L as well as the magnetizing current i_{mag} as shown in Figure 2.4. The voltage over the switch V_T is twice the input voltage while the transformer demagnetizes, during the off cycle, as shown in Figure 2.4.
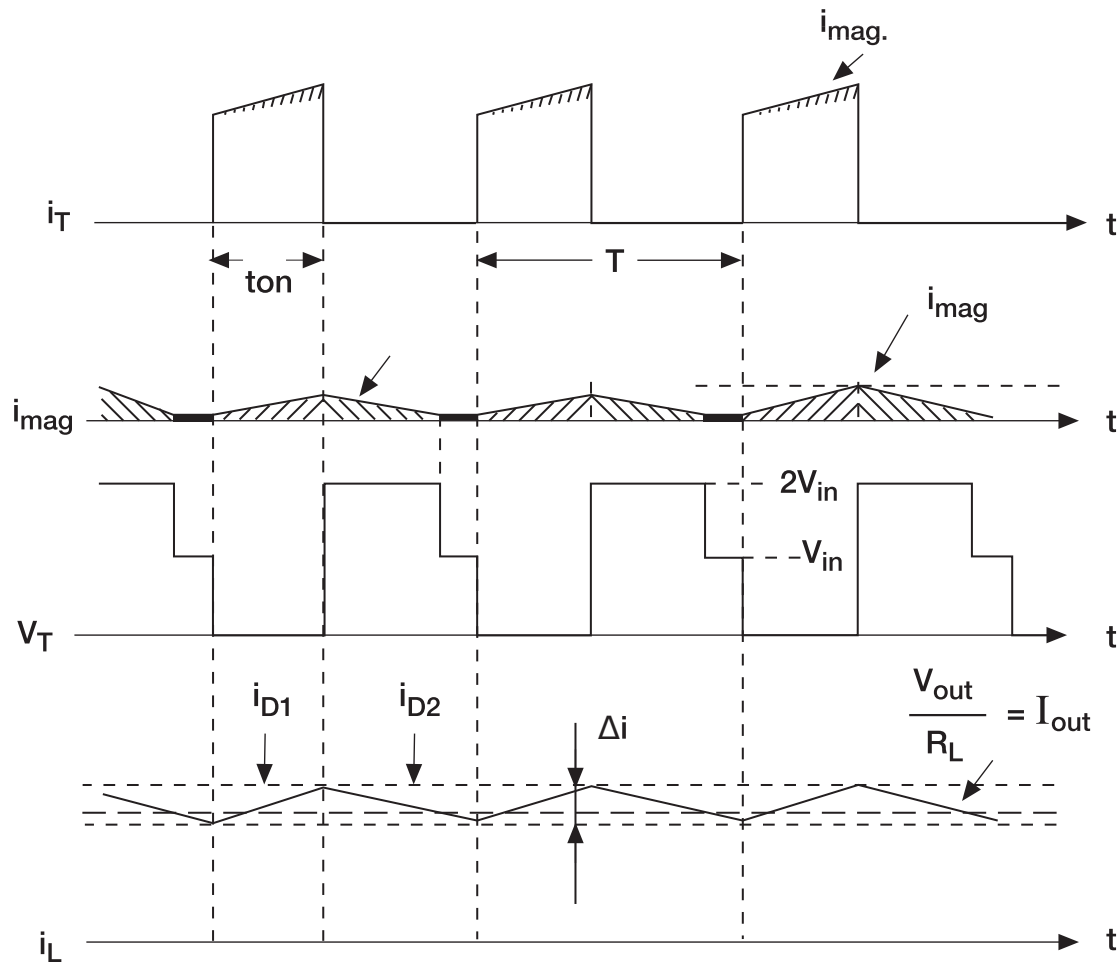
Figure 2.4. Forward topology waveforms [19].

2.3.3 Double switch forward topology

The double switch forward topology, shown in Figure 2.5, is a refined version of the single switch forward topology. This topology has two switches, one on the high side and one on the low side of the transformer [23]. This eliminates the need for a reset winding and also enables the use of a lower voltage and faster switching MOSFETs because the switches only have to withstand the input voltage [19, 23, 24]. The transformer is demagnetised through the demagnetisation diodes on the primary side [19].

The total current i_T flowing through the switch and primary windings of the transformer is the reflected output inductor current i_L as well as the magnetizing current i_{mag} as shown in Figure 2.6. The
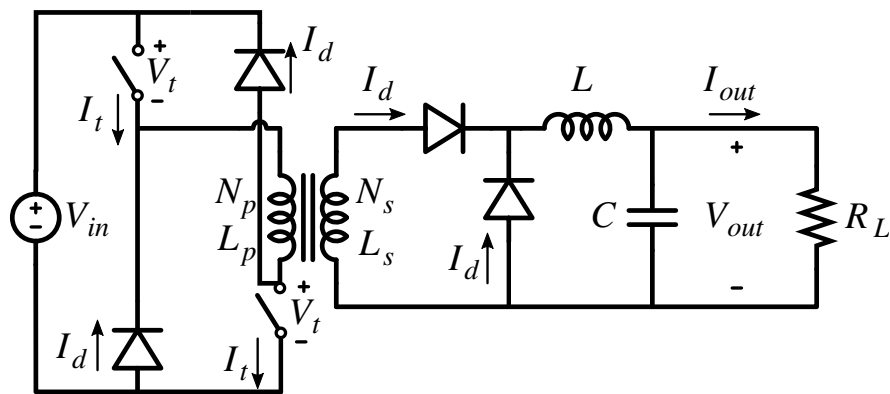
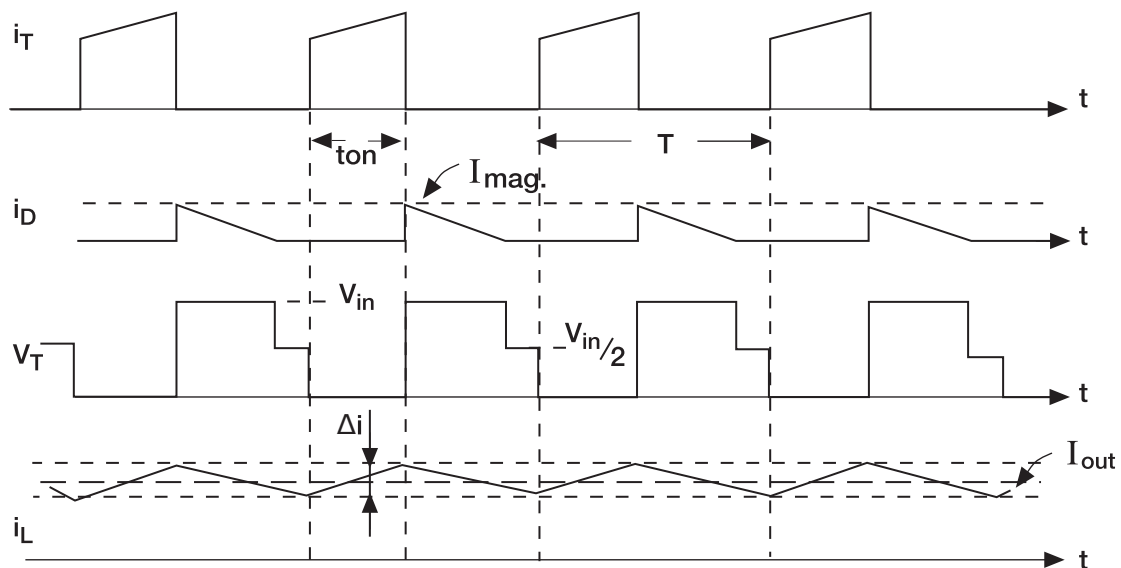**Figure 2.5.** Double switch forward topology [19].

Figure 2.6. Double switch forward topology waveforms [19].

magnetization current i_{mag} flowing through the diodes on the primary side of the transformer to reset the core is shown in Figure 2.6. The voltage across the switches V_T is the input voltage while the magnetization current is not zero during the off period and once the core has been reset the voltage over the switches is half the input voltage as shown in Figure 2.6.

2.3.4   Half bridge topology

The half bridge topology, shown in Figure 2.7, has a distinct advantage over the forward and flyback converters because it has two bulk input capacitors that divide the input voltage by two. This means
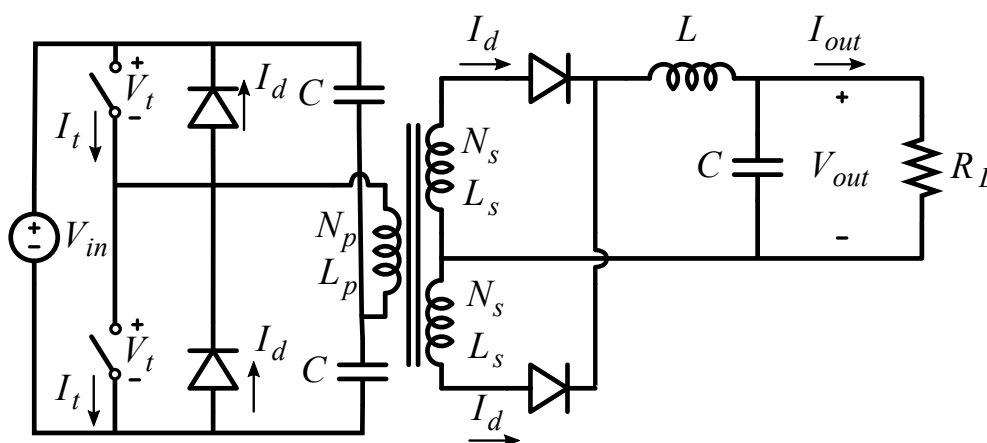
Figure 2.7. Half bridge topology [19].

that the primary switching devices have a lower voltage rating and thus operate at higher switching frequencies [19, 23, 24]. The clamp diodes on the primary side of the converter help to protect the switching devices from leakage inductance and magnetisation voltage spikes by directing these voltages back to the two input capacitors [19, 23, 24]. This topology has a low output voltage ripple because the transformer current is continuous. The half bridge topology is typically used for the application where 500 W up to 1 kW of power is required [19, 23, 24].

The current flowing through the switch i_{T1} is equal to the sum of the reflected secondary current and the primary magnetizing current. This is true for both switches and is shown in Figure 2.8. The voltage over the output inductor is equal to the difference between the primary voltage reflected to the secondary side and the output voltage. This applied voltage is in the forward direction and accounts for the linear rise in the inductor current i_L as shown in Figure 2.8. When both switches are off half of the inductor current i_L is flowing through each of the two secondary rectifying diodes i_{D1} and i_{D2} as shown in Figure 2.8. This causes an equal and opposite voltage being applied to the transformer secondary windings, thus causing a net zero voltage over the secondary side of the transformer which keeps the flux density in the transformer core constant. When both switches are off the output voltage is applied over the inductor in a reverse direction causing the inductor current i_L to decrease as shown in Figure 2.8. The voltage over the switches V_T and V_T are shown in Figure 2.8, where it can be seen that each switch only needs to withstand the input voltage.
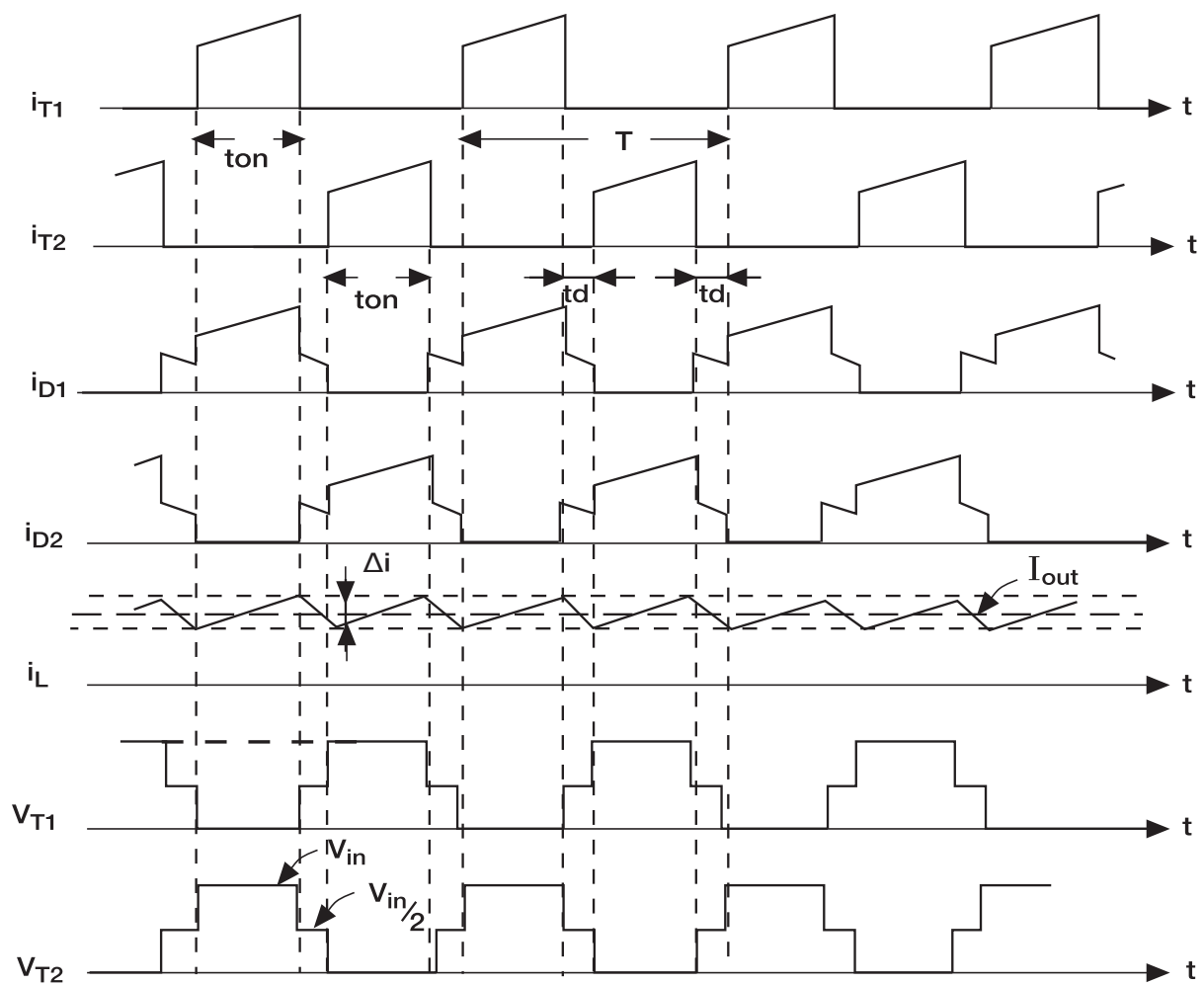
Figure 2.8. Half bridge topology waveforms [19].

2.3.5   Full bridge topology

The full bridge topology, shown in Figure 2.9, is normally used in applications where high output power is required. This converter can supply power from 500 W up to 2 kW [23, 24]. It is, however, complex to design and construct because a full square wave has to be generated. Small signal isolation transformers have to isolate the controller from the high side switching devices because these devices have a floating source [19, 23, 24]. This converter, however, makes the best use of the transformer for the reason that the latter is fully magnetised and demagnetised in each half of the duty cycle, thus producing high output power with low output voltage ripple [23].

The current flowing through the switch pair i_{T1} and i_{T3} is equal to the sum of the reflected load current
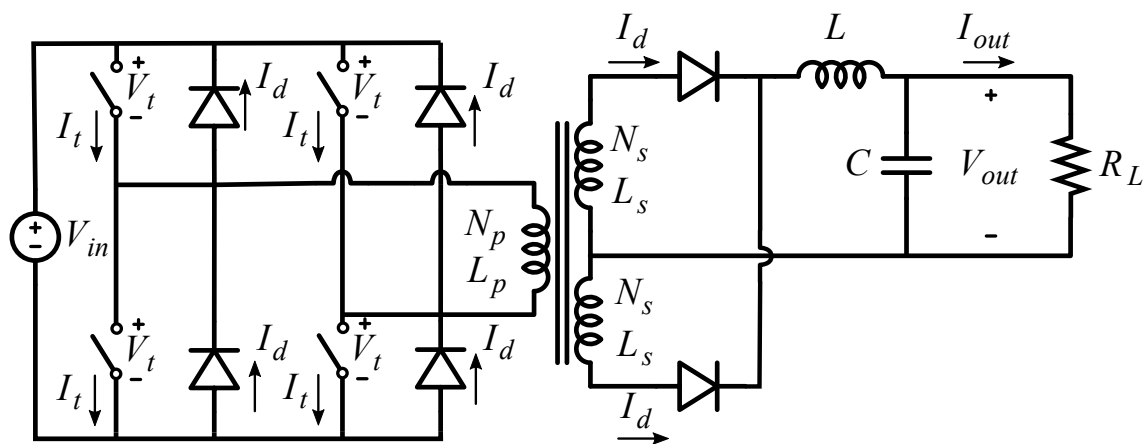
Figure 2.9. Full bridge topology [19].

and the primary magnetizing current. This is true for both switch pairs and is shown in Figure 2.10.The

voltage over the output inductor is equal to the difference between the primary voltage reflected to the

secondary side and the output voltage. This applied voltage is in the forward direction and accounts for

the linear rise in the inductor current i_L as shown in Figure 2.10. When both switch pairs are off half

of the inductor current i_L is flowing through each of the two secondary rectifying diodes i_{D1} and i_{D2}

as shown in Figure 2.10. This causes an equal and opposite voltage being applied to the transformer

secondary windings, thus causing a net zero voltage over the secondary side of the transformer which

keeps the flux density in the transformer core constant. When both switch pairs are off the output

voltage is applied over the inductor in a reverse direction causing the inductor current i_L to decrease

as shown in Figure 2.10. The voltages over the switch pairs $V_{T1,3}$ and $V_{T2,4}$ are shown in Figure 2.10,

where it can be seen that each switch only needs to withstand the input voltage.

2.4   NON-ISOLATED SWITCH-MODE TOPOLOGIES

The non-isolated topologies are discussed in this section to identify the benefits and shortfalls of each.

A brief circuit description with critical waveforms is also presented for each of the topologies.

2.4.1   Buck converter topology

The buck converter topology, shown in Figure 2.11, is used to step voltages down by varying the duty

cycle of the switching transistor or MOSFET [19, 23, 24]. This topology has low output ripple because
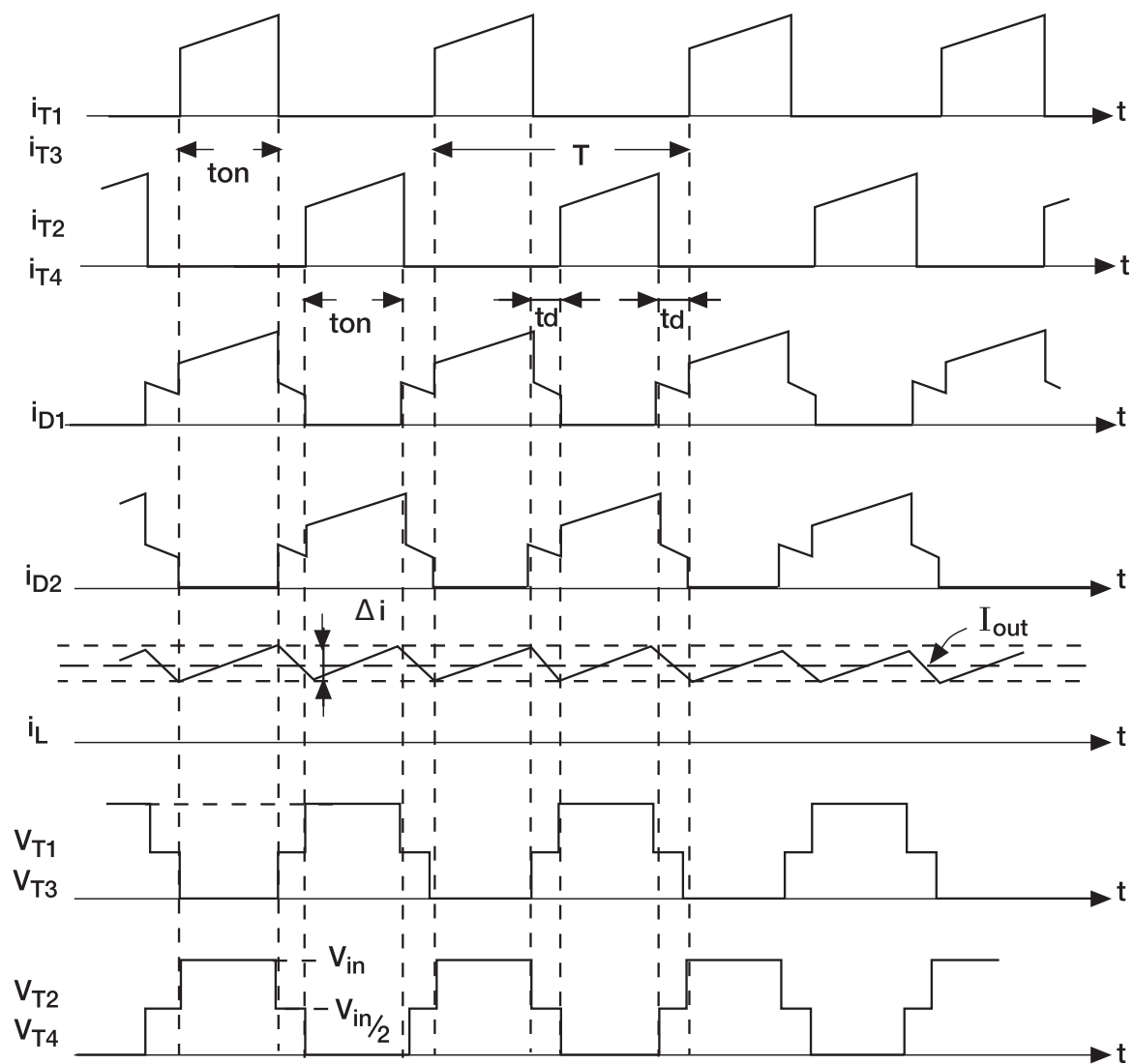
Figure 2.10. Full bridge topology waveforms [19].

the output current is continuous [24]. It means that the output filter of this converter can be small in comparison to the next two converters. This topology also has a small footprint when compared to an isolated topology.

During normal operation when the switch is on, during the on period, the input energy source supplies energy to the output as well as the inductor. When the switch is on the current flows through the inductor to the output. The difference between the input and output voltage is the voltage applied over the inductor during the on period. It can be seen in Figure 2.12 that the inductor current i_L rises linearly with the current i_T through the switch. When the switch is turned off, during the off period, the output is supplied with current stored in the inductor. Once the switch is turned off the output
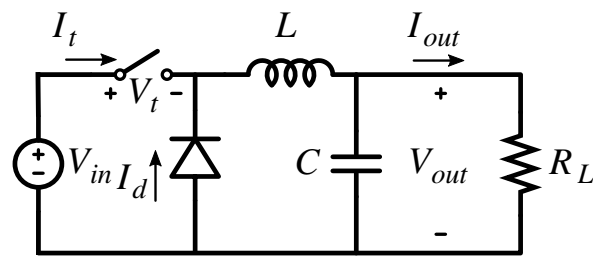
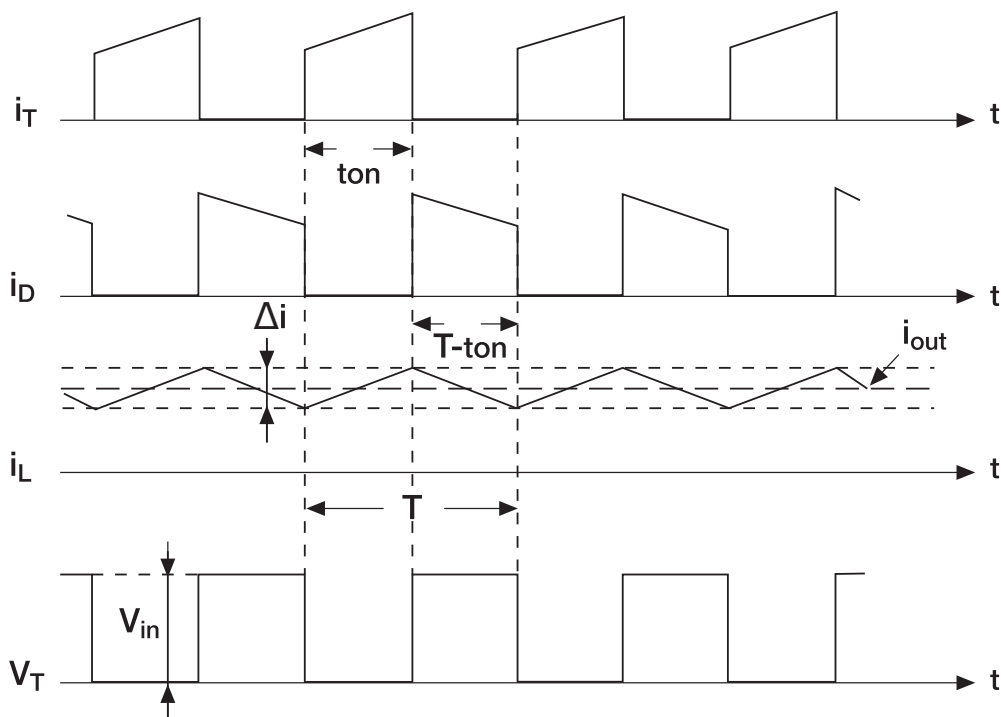**Figure 2.11.** Buck converter topology [19].

Figure 2.12. Buck converter topology waveforms [19].

voltage is applied in a reverse direction over the inductor thus accounting for the decreasing current flow through the inductor. Figure 2.12 shows that the current starts to flow through the diode i_D and that the current flow through the inductor decreases during the off period. During the off period the input voltage is applied over the switch V_T as shown in Figure 2.12.

2.4.2 Boost converter topology

The boost converter topology, shown in Figure 2.13, is used to step voltages up by varying the duty cycle of the switching transistor or MOSFET [19, 23, 24]. This topology tends to have a large amount
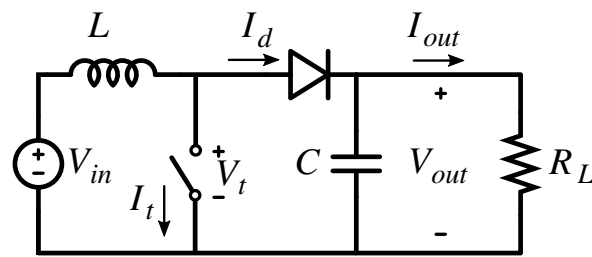
Figure 2.13. Boost converter topology [19].

of output ripple since the output current is discontinuous [19, 23, 24]. A large output capacitor is, therefore, needed to reduce the output ripple and to produce a stable DC output voltage.

The input energy source feeds the output through the inductor and diode when the switch is off. During the on period, energy is stored in the inductor since the input voltage is applied in a forward direction to the inductor. Figure 2.14 shows that the inductor current i_L increases during the on period along with the current i_T through the switch. The output current through the load is supplied by the output capacitor during the on period. When the switch is off, during the off period, the difference between the input and output voltage is applied in a reverse direction to the inductor, thus accounting for the decreasing current flow through the inductor. Figure 2.14 shows that the current i_D starts to flow through the diode and that the current through the inductor decreases during the off period. During the off period the output voltage is applied over the switch V_T as shown in Figure 2.12.

2.4.3   Buck-boost converter topology

The buck-boost converter topology, shown in Figure 2.15, combines the buck and boost converters to either step a voltage up or down, depending on the duty cycle [19, 23, 24]. When the duty cycle is below 0.5, the converter will step the voltage down and when the duty cycle is above 0.5, the converter will step the voltage up. This topology tends to have a higher output voltage ripple than the buck converter and less than the boost converter and, therefore, requires a large output filter to reduce the output voltage ripple [19, 23, 24].

During the on period, energy is stored in the inductor since the input voltage is applied in a forward direction to the inductor and the output capacitor supplies the output current to the load. Figure 2.16 shows that the inductor current i_L increases during the on period along with the current i_T through
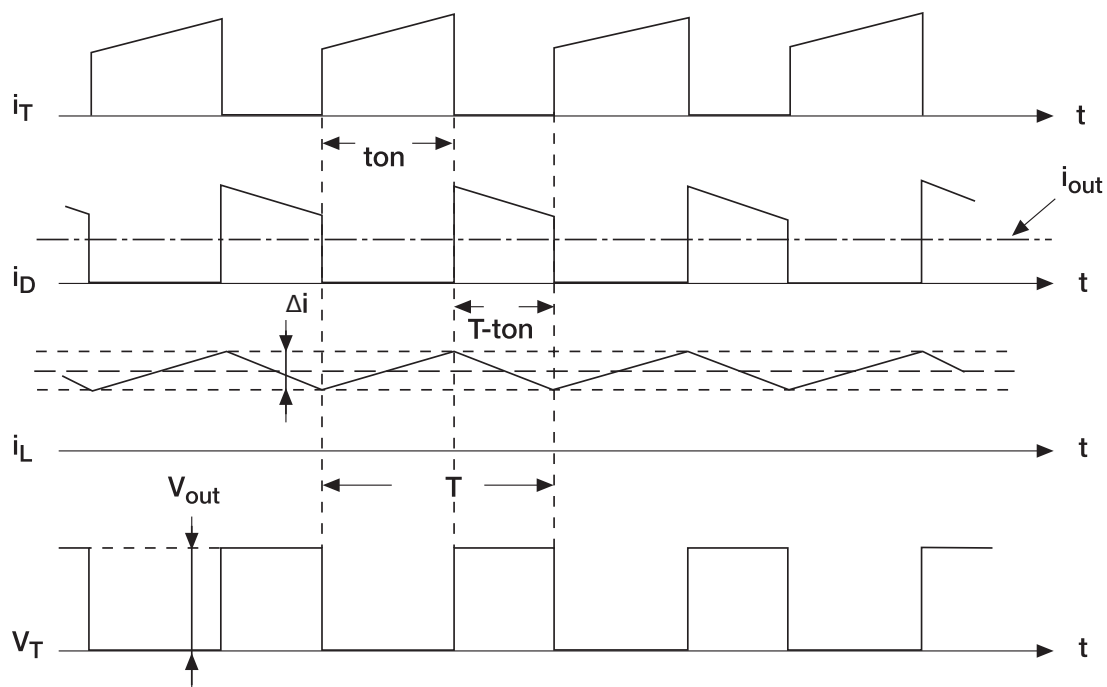
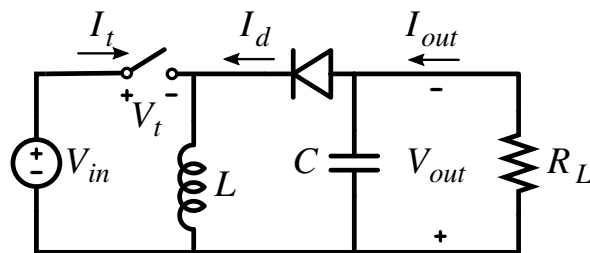**Figure 2.14.** Boost converter topology waveforms [19].

Figure 2.15. Buck-Boost converter topology [19].

the switch. When the switch is off, during the off period, the difference between the input and output voltage is applied in a reverse direction to the inductor, thus accounting for the decreasing current flow through the inductor. Figure 2.16 shows that the current i_D starts to flow through the diode and that the current through the inductor decreases during the off period. During the off period the sum of the input and output voltages are applied over the switch V_T as shown in Figure 2.16.

2.5   SWITCH-MODE TOPOLOGY SELECTION

A typical valve amplifier has one low voltage output of 6.3 V to supply the valve heaters, one high voltage output of up to 450 V to supply the valve plates and output transformer and sometimes a
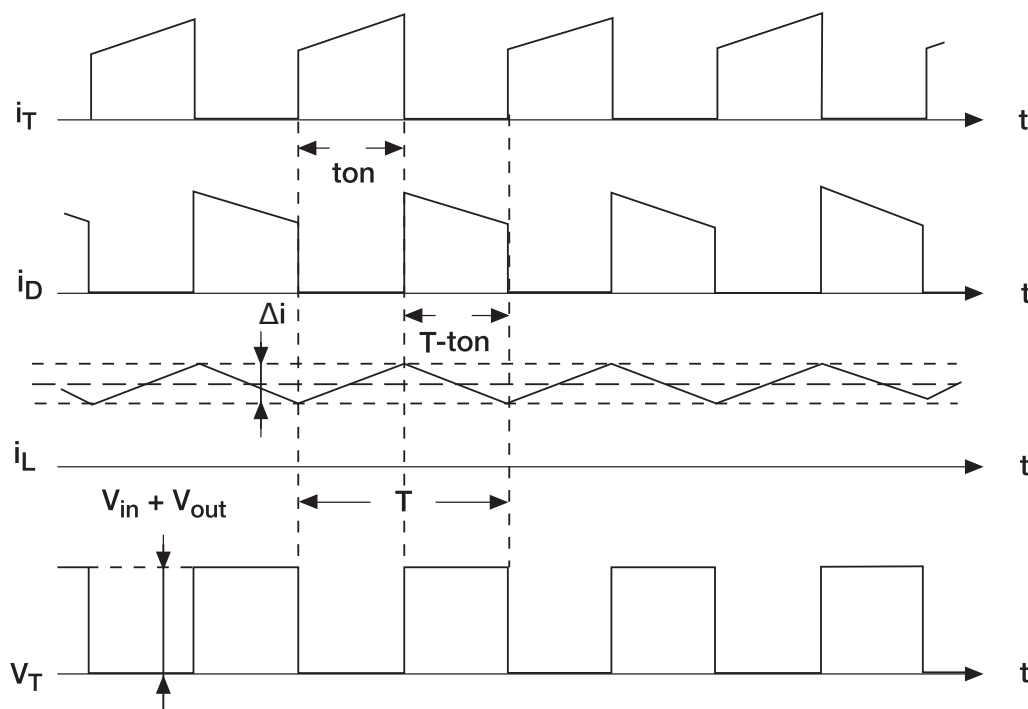
Figure 2.16. Buck-Boost converter topology waveforms [19].

medium voltage output of down to -60 V to supply the bias point to the power amplifier section [6, 7].
Since only three different output voltages have to be generated, separate boost and buck converters
with a common isolation stage are a sensible choice. This choice is based on the fact that the valve
amplifier will have exposed conductive parts and, therefore, requires an isolated power supply. Three
separate power supply sections are needed to independently adjust each output voltage and to obtain a
different output response for each of the outputs. To generate the three separate outputs, two possible
options are available. Each option is discussed below.

Option 1: Three separate forward converters can be used to generate the three independent output
voltages. This option will give independent control of each output without affecting the other.
This would also allow developing each section separately with an integration phase afterwards.
This option would result in a slightly bigger form factor than Option 2 and at a slightly higher
cost.

Option 2: One isolation stage with one boost and two buck converters connected to its output to
generate the independent outputs. The three outputs would not be totally independent of one
another since the forward converter can saturate and affect the output voltages of all three outputs,

but this should not be a problem since the boost and buck converters can compensate for slight input voltage variations to keep the output voltage as stable as possible. This option would result in a slightly smaller form factor since only one transformer is needed.

Option 2 was selected since the design is not as complicated when compared to the other option and will still be able to comply with the design requirements. This option would also provide more freedom to change the feedback loops and output impedance to obtain the required output response from the power supply without having to test different transformer designs.

2.6   CHAPTER CONCLUSION

From this chapter, it can be concluded that a switch-mode power supply will result in a significantly lighter amplifier which will also be smaller and easier to handle. There are also different switch-mode power supply topologies that can be used to optimise the design for cost, efficiency and size. These factors can be weighted and then used to select a suitable topology with a minimal design trade-off.

CHAPTER 3   BOOST CONVERTER MODULE AND AUXILIARY CIRCUIT DESIGNS

3.1   CHAPTER OBJECTIVES

The boost converter design is shown in this section. The equations in this section show the component values for the designed switch-mode power supply. The assumptions that were made during the design are also stated here. The two buck converters were excluded from this study since the selected valve amplifier does not need a negative bias voltage and the valve heater voltage does not have an impact on the amplifier, except for additional hum added to the output if an AC heater voltage is used. Because of this, only the boost converter needs to be constructed and tested in this study. The isolation stage was accomplished with the use of an isolation transformer since the isolation stage will not have an impact on the regulated output of the boost converter.

3.2   BASIC OPERATION

The non-isolated power factor corrected boost converter topology was selected for this study. This converter operates in a frequency clamped critical conduction mode and performs well in low power applications with good light load performance. It also has a fixed frequency range that requires a less complicated EMI filter design because of lower core losses and relaxed filter requirements when compared to a critical conduction mode converter with no frequency clamp limits. Figure 3.1 shows the current through the boost converter inductor for the three different operating modes. From this figure, it can be seen that when the controller is operated in the continuous conduction mode the switch is turned on again during the ramp down cycle and thus ensuring that the current flow through the inductor never reaches zero. When the controller is operated in the discontinuous conduction mode the
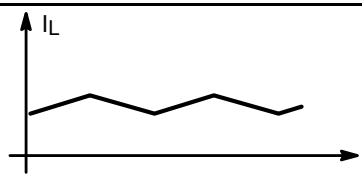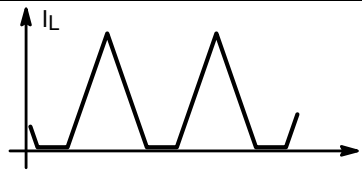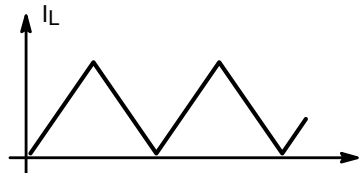
Rating	Symbol
I_L (waveform)	**C**ontinuous **C**onduction **M**ode (CCM)
I_L (waveform)	**D**iscontinuous **C**onduction **M**ode (DCM)
I_L (waveform)	**Cr**itical **C**onduction **M**ode (CrM)

Figure 3.1. Operating mode comparison [25].

current through the inductor reaches zero and has some dead time before the switch is turned on again. And when the controller is operated in the critical conduction mode the switch turns on immediately when the current through the inductor reaches zero, thus having no dead time.

The critical conduction mode is widely used in power supply designs but has some limitations. The biggest limitation is the variable switching frequency of the controller. The switching frequency is the highest at light loads and also near the zero crossing of the sinusoid. Ons solution to this problem is to clamp the switching frequency between upper as well as lower limits. Once the frequency is clamped at the upper limit, under low load conditions, the output current of the converter becomes distorted since the on time is not properly adjusted. Once the switching frequency is clamped at the upper limit the inductor enters the discontinuous mode of operation which also lowers the power factor of the power supply. One solution to this problem is to use a controller that operates in the critical conduction mode but also perform power factor correction in the discontinuous conduction mode when the switching frequency is clamped. This solution will allow the controller to switch to the discontinuous conduction mode at light loads to avoid the high switching frequencies of the critical conduction mode. At higher loads, the controller will switch to the critical conduction mode to avoid the higher peak currents generated through the inductor when operating in the discontinuous conduction mode. This is illustrated in Figure 3.2. The critical conduction mode also has an intrinsically stable current loop and therefore do not need ramp compensation to be implemented, thus making the control
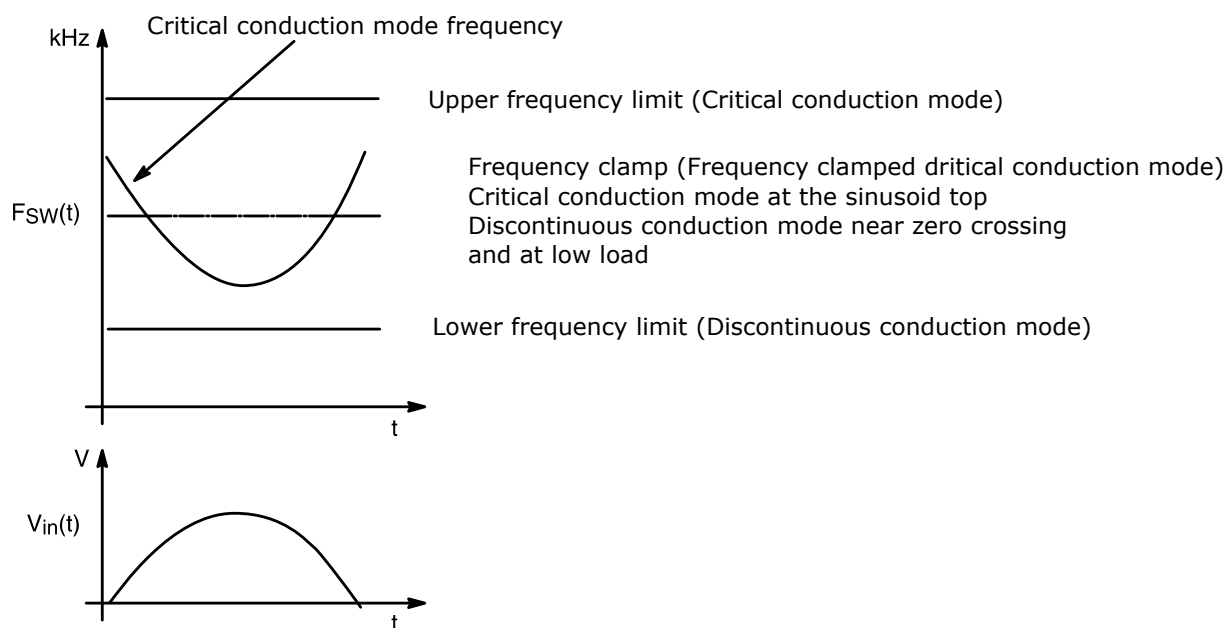
Figure 3.2. Operating mode selection [25].

a bit simpler.

A simplified schematic of a critical conduction mode boost converter is shown in Figure 3.3. The controller has a built-in error amplifier with a low-frequency pole that provides an error signal to the reference multiplier. The reference multiplier also receives a scaled-down version of the full wave rectified AC voltage as an input. The reference multiplier then provides an output signal from the product of the error signal and the scaled down rectified AC signal. The output of the reference multiplier is fed to the current shaping network. The current shaping network is used to force the input current flow to follow the output of the reference multiplier, thus ensuring that the input current is not distorted and stays in phase with the input voltage. Figure 3.4 show the working of the current shaping network, where the reference voltage is the output of the reference multiplier, the average input current and current through the inductor is also shown. The current shaping network functions by turning on the MOSFET, the current ramps up until the threshold voltage over the current sense resistor is reached. The MOSFET is then turned off until the current through the inductor reaches zero. The MOSFET is turned on again once the zero current detection circuit detects that the current through the inductor reached zero. This control method ensures that the wave shape of the current through the inductor is known and therefore ensures that the relationship between the average and peak current is also known. For the triangular waveform of the current through the inductor, the average current is half of the peak current as shown in Figure 3.4. From Figure 3.4 it can also be seen that the switching
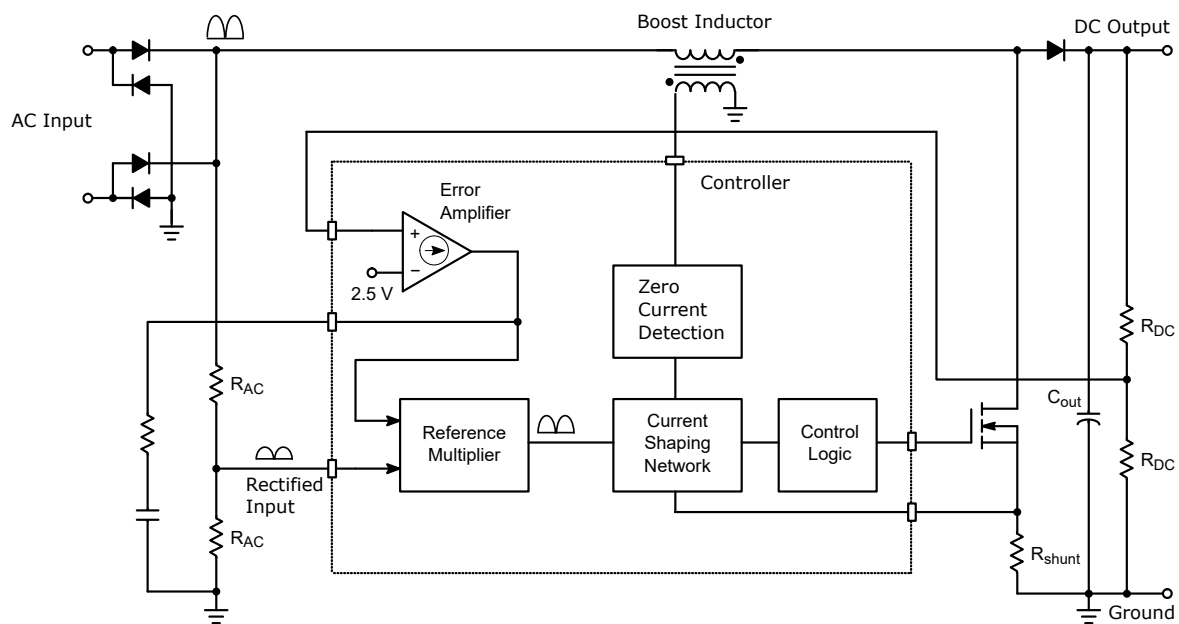
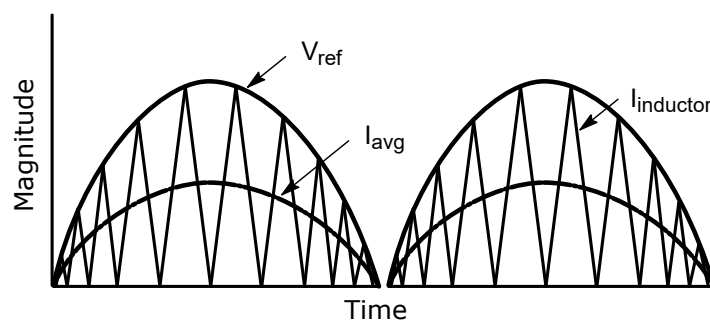**Figure 3.3.** Critical conduction mode boost converter schematic [25].

Figure 3.4. Critical conduction mode boost converter waveforms [25].

frequency will be much higher near the zero crossing.

Once the switching frequency is clamped at the high limit, under high line voltages with light loads or near the zero crossing, the controller will transition into a discontinuous conduction mode where the current through the inductor will stay zero for a determined amount of time during the duty cycle as shown in Figure 3.5. The discontinuous conduction mode can be divided into 3 phases. The first phase is with the switch on and current is flowing through the inductor, the second phase is with the switch off while current is still flowing through the inductor and the third phase is with the switch off with no current flowing through the inductor.
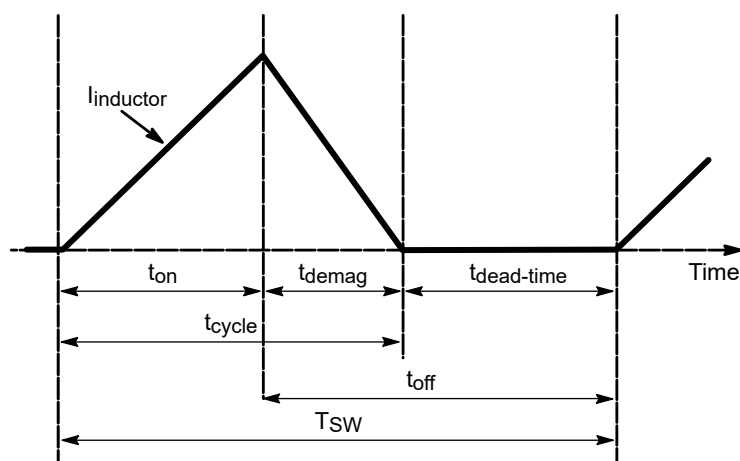
Figure 3.5. Discontinuous conduction mode operating waveforms [25].

3.2.1   Voltage feedback loop

To implement a voltage feedback loop, two inputs are required. Firstly, a measurement of the power supply output voltage and, secondly, a reference voltage. The voltage measurement power supply output could then be compared to the reference voltage. Based on the comparison, the pulse width modulation (PWM) frequency of the controller could be adjusted to raise or lower the output voltage relative to the reference voltage. The comparator feedback voltage, V_X, could be calculated using (3.1) with the reference voltage being V_{ref} and the feedback voltage from the power supply being V_{fb}. The comparator feedback voltage could either be used to provide feedback to a PWM controller or to a second comparator to compare the comparator feedback voltage, V_X, to a sawtooth signal generating a PWM signal which can be used to control the primary driving circuit.

$$V_X = V_{ref} - V_{fb} \tag{3.1}$$

The implementation of a voltage feedback loop is fairly simple and it is effective in handling disturbances. Voltage feedback loops also have larger amplitude signals which help with noise margins in the circuitry. This feedback loop, however, has the disadvantage of a delay when the input or output voltage of the power supply changes because of inductors present in the output circuit of the power supply. The biggest delay is a change in the input voltage since this disturbance has to propagate through the circuit to the output to be detected and then has to be compensated for.

How to compensate for changes or disturbances in the input and output voltage of the power supply, are discussed below.

3.2.1.1 Line regulation

Line regulation refers to how the power supply reacts to changes in the input voltage. The controller has to compensate for these changes to ensure that the output of the power supply is as stable as possible. When the input voltage of the power supply increases, so does the average output current on the secondary side of the power supply. This leads to a higher output voltage. To compensate for this, the PWM duty cycle has to be lowered in order to lower the output voltage. To handle this disturbance more accurately, a voltage measurement of the input voltage to the power supply has to be used in a feed-forward control loop.

3.2.1.2 Load regulation

Load regulation refers to how the power supply reacts to changes in the output load. If the load, R_O, of the power supply lowers in resistance, the output voltage will decrease. To compensate for this, the controller has to increase the PWM duty cycle to raise the output voltage. In order to handle this disturbance, a measurement of the power supply output voltage has to be used in a feedback loop.

3.2.2 State space model

The state space model of the boost converter during the on period can be derived from Figure 3.6 by applying Kirchhoff's voltage law to the input loop and Kirchhoff's current law to the output loop, shown in (3.2) and (3.3) respectively. The output voltage, V_o can be approximated by (3.4). The state space model of the boost converter is given by (3.5) and (3.6) by taking (3.4) into account and rewriting (3.2) and (3.3).

$$V_s = i_L r_L + L\frac{di_L}{dt} + V_o(1-D) \tag{3.2}$$

$$i_L(1-D) = C\frac{dv_c}{dt} + \frac{V_o}{R} \tag{3.3}$$

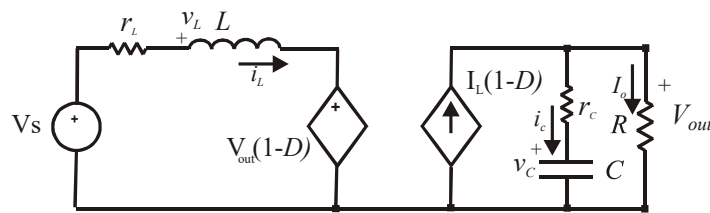$$V_o = r_c i_c + v_c \approx v_c \tag{3.4}$$

Figure 3.6. Boost converter linear equivalent circuit diagram.

$$\frac{di_L}{dt} = \frac{i_L r_L}{L} - \frac{v_c}{L}(1-D) + \frac{V_s}{L} \tag{3.5}$$

$$\frac{dv_c}{dt} = \frac{i_L}{C}(1-D) - \frac{v_c}{R \cdot C} \tag{3.6}$$

3.3   DESIGN EQUATIONS

The following parameters had to be defined before the boost converter circuit could be designed.

- Maximum input voltage: $V_{ac,max}$ = 264 V_{ac}
- Minimum input voltage: $V_{ac,min}$ = 88 V_{ac}
- Line frequency: f_{line} = 50 Hz
- Output voltage: V_{out} = 430 V_{dc}
- Maximum output voltage: $V_{out,max}$ = 440 V_{dc}
- Output power: P_{out} = 50 W
- Minimum switching frequency: $f_{sw,min}$ = 55 kHz
- Maximum switching frequency: $f_{sw,max}$ = 80 kHz
- Output voltage ripple: $V_{ripple(p-p)}$ = 16 V
- Hold up time: t_{holdup} = 16 ms
- Estimated efficiency: η = 93%

The inductor size normally depends on the root-mean-square (RMS) current through it as well as the inductance value. The core losses tend the be higher with higher peak to peak currents flowing through the inductor in the critical conduction mode. This makes the core selection critical to ensure that the power supply will function correctly and efficiently. The current through the inductor is at the maximum when the input voltage of the power supply is at the minimum in order to deliver the same amount of power when compared to high input voltages. The input current can be assumed to be

constant during each switching period since the switching frequency is much higher than the input line frequency. The peak current through the boost inductor $I_{coil,pk}$ is given by (3.7), the RMS current through the inductor $I_{coil,RMS}$ is given by (3.10). The inductance of the inductor L was calculated using (3.13). The minimum line voltages were used for these calculations since these conditions will put the most stress on the power supply and thus yield the worst case situation.

$$I_{coil,pk} = \frac{2\sqrt{2}P_{out}}{\eta V_{ac,min}} \tag{3.7}$$

$$= \frac{2 \cdot \sqrt{2} \cdot 30}{0.93 \cdot 88} \tag{3.8}$$

$$= 1.04 \text{ A} \tag{3.9}$$

$$I_{coil,RMS} = \frac{I_{coil,pk}}{\sqrt{6}} \tag{3.10}$$

$$= \frac{1.04}{\sqrt{6}} \tag{3.11}$$

$$= 0.42 \text{ A} \tag{3.12}$$

$$L \geq \frac{\eta \left(V_{ac,min}\right)^2 \left(\frac{V_{out}}{\sqrt{2}} - V_{ac,min}\right)}{\sqrt{2}V_{out}P_{out}f_{sw,min}} \tag{3.13}$$

$$L \geq \frac{0.93 \cdot 88^2 \left(\frac{430}{\sqrt{2}} - 88\right)}{\sqrt{2} \cdot 430 \cdot 30 \cdot 55000} \tag{3.14}$$

$$L \geq 1.50 \text{ mH} \tag{3.15}$$

The minimum number of turns on the inductor $N_{B,min}$ are given by (3.16). The cross-section area of the inductor core is given by A_e and the saturation flux density in Tesla is given by B_{sat}.

$$N_{B,min} = \frac{LI_{coil,pk}}{B_{sat}A_e} \cdot 10^6 \tag{3.16}$$

$$= \frac{1.5 \cdot 10^{-3} \cdot 1.04}{0.32 \cdot 125} \cdot 10^6 \tag{3.17}$$

$$= 39 \text{ turns} \tag{3.18}$$

Choose N_B as 40 turns.

The oscillator capacitor capacitance C_{osc} was calculated using (3.19). The charge current of the capacitor I_{charge} and voltage variation $\triangle V$ were obtained from the driver datasheet. This capacitor is used to set the maximum switching frequency of the converter. This frequency will be used to switch

to the discontinuous conduction mode.

$$C_{osc} = \frac{I_{charge}}{2\,\Delta V\,f_{sw,max}} - 20 \cdot 10^{-12} \tag{3.19}$$

$$= \frac{100 \cdot 10^{-6}}{2 \cdot 1 \cdot 80000} - 20 \cdot 10^{-12} \tag{3.20}$$

$$= 605 \text{ pF} \tag{3.21}$$

The current sense resistor can also easily increase the conduction losses if the resistance is to high. The voltage drop over the current sense resistor at full load should also be minimised. For these reasons the current sense resistor is chosen as $0.1\ \Omega$. The current sense resistor R_{sense} was used to calculate the current feedback resistor $Rocp$ using (3.22). The feedback current $I_{pin5,max}$ was obtained from the driver datasheet. The voltage over the current sense resistor is a negative voltage that can be converted into a current signal when a resistor is placed between the current sense resistor and the signal pin of the controller.

$$R_{ocp} = \frac{I_{coil,pk}R_{sense}}{I_{pin5,max}} \tag{3.22}$$

$$= \frac{1.04 \cdot 0.1}{250 \cdot 10^{-6}} \tag{3.23}$$

$$= 416\ \Omega \tag{3.24}$$

The termination resistor for the zero cross detection R_{ZCD} was chosen to be three times that of R_{ocp}. The drive resistor R_{DRV} was chosen to be three times that of R_{ZCD} and is used to implement hysteresis in the zero cross detection circuit. $R_{ZCD} = 1.25\ \text{k}\Omega$ and $R_{DRV} = 3.74\ \text{k}\Omega$.

The zero crossing detection winding is used to detect the zero current mark of the boost inductor. The auxiliary winding should be designed to provide enough energy to trigger the zero crossing detection threshold in order to detect zero current. The winding ratio between the boost inductor winding N_B and zero cross detection winding N_{ZCD} were calculated using (3.25). The value of R_{ZCD1} was chosen to be two times that of R_{ZCD}. The high level of the zero cross detection voltage V_{ZCDH} was obtained

from the datasheet.

$$\frac{N_B}{N_{ZCD}} \leq \frac{\left(V_{out} - \sqrt{2}V_{ac,max}\right)}{V_{ZCDH}\frac{R_{ZCD}+R_{ZCD1}}{R_{ZCD}} + V_f} \tag{3.25}$$

$$\frac{N_B}{N_{ZCD}} \leq \frac{\left(430 - \sqrt{2}\cdot 264\right)}{0.1\cdot 3 + 0.3} \tag{3.26}$$

$$\frac{50}{N_{ZCD}} \leq 44.4 \tag{3.27}$$

$$N_{ZCD} = 2 \text{ turns} \tag{3.28}$$

Choose R_{ZCD1} to be 2.5 kΩ.

The voltage feedback circuit is comprised of a voltage divider to feed the output voltage back to the controller in order to regulate the output voltage. This voltage feedback option was chosen since it is a bit slower than a current feedback loop and thus allows the output voltage to sag a bit before the controller takes action to compensate for this. The output voltage is set by using the voltage divider to lower the output voltage to match the required reference voltage that the controller expects. The regulation stage of the controller has a low bandwidth which means that the controller will have a sluggish response to sudden changes of the output voltage. This sluggish response results in a undershoot of the output voltage when there is a sudden current demand on the output of the power supply. When the output voltage of the power supply is too far from the regulation level an internal current source is connected to the output of the internal feedback comparator to speed up the regulation loop. The gain of the error amplifier is effectively multiplied by roughly 10 when the 200 μA current source is connected to the compensation pin. This help to avoid the controller going into an under voltage protection mode in which the controller will switch off. The internal feedback section is a transconductance error amplifier with a typical transconductance gain of 200 μS and a maximum internal capacitance of 20 μF, shown in Figure 3.7. The scaled down output voltage is connected to the inverting input of the amplifier, FB, and the reference voltage is connected to the non-inverting input of the amplifier. The output of the transconductance amplifier, $V_{control}$, is then connected to an output for external loop compensation to set the regulation bandwidth of the power supply. The over voltage protection section of the controller limits the amount of overshoot since the bandwidth of the regulation section was set very low to obtain the required undershoot on the output of the power supply. From Figure 3.7 it can be seen that the output of the error amplifier is kept above the voltage drop over a diode, V_F, and is clamped to not exceed the sum of V_F and 3 V. The external loop compensation output thus has a voltage swing of 3 V. The output of the error amplifier is then offset down by V_F and
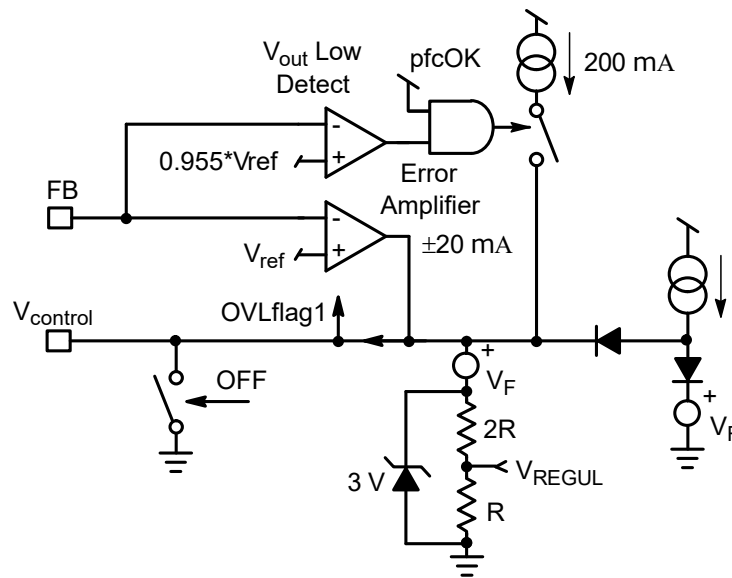
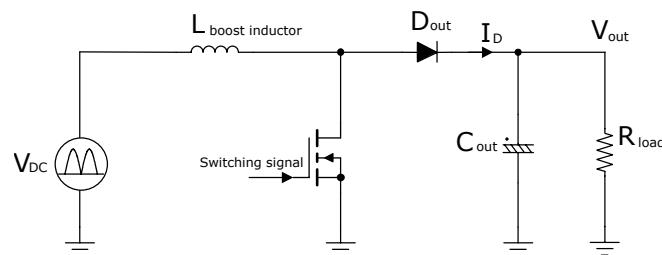**Figure 3.7.** Controller internal feedback section [25].

Figure 3.8. Boost converter power stage.

then divided by three before being outputted to the PWM section of the controller to provide a control signal that varies between 0 and 1 V.

The compensation network is used to adjust the bandwidth of the power supply. The main power stage of the boost converter is shown in Figure 3.8. The small signal model of the power stage is shown in Figure 3.9. The diode and MOSFET were replaced by loss free resistor models and can then be modelled as a voltage controlled current source that is feeding an RC network. The low-frequency behaviour of the voltage controlled current source is obtained by averaging the diode current during a half line cycle and is given by (3.29) where K_{SAW} is the gain of the internal sawtooth generator. The control to output transfer function of the small signal low-frequency model is given by (3.30) with R_L the output load resistance.
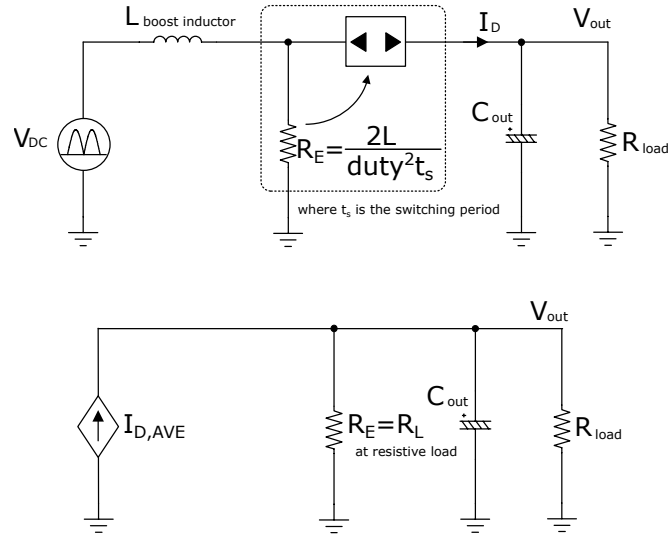
Figure 3.9. Boost converter small signal model.

$$I_{Dout,AVE} = K_{SAW} \cdot \frac{\sqrt{2}V_{Line}}{4V_{out}} \cdot \frac{\sqrt{2}V_{Line}}{L} \tag{3.29}$$

$$\frac{V_{out}}{V_{comp}} = K_{SAW} \cdot \frac{V_{Line}^2 R_L}{4V_{out} \cdot L} \cdot \frac{1}{1 + \frac{s}{2\pi f_p}} \tag{3.30}$$

where

$$f_p = \frac{2}{2\pi \cdot R_L C_{out}}. \tag{3.31}$$

The DC gain and crossover frequency, f_c of the control loop increases as the input voltage increase. The DC gain also increases as the load decreases. As a result of this the worst conditions for feedback loop design will be high input voltages and light load conditions. To compensate for this proportional and integral control can be implemented. The compensation loop will add a low frequency zero and a high frequency pole to the control loop. The compensation zero introduced phase boost and the high frequency pole attenuates the switching noise. The compensation network transfer function is given by (3.32).

$$\frac{V_{out}}{V_{comp}} = \frac{2\pi f_I}{s} \cdot \frac{1 + \frac{s}{2\pi f_{cz}}}{1 + \frac{s}{2\pi f_{cp}}} \tag{3.32}$$

with

$$f_I = \frac{2.5}{V_{out}} \cdot \frac{115\mu mho}{2\pi \cdot (C_{comp,lf} + C_{comp,hf})} \tag{3.33}$$

where

$$f_{cz} = \frac{1}{2\pi \cdot R_{comp} \cdot C_{comp,lf}} \tag{3.34}$$

$$f_{cp} = \frac{1}{2\pi \cdot R_{comp} \cdot \frac{C_{comp,lf} \cdot C_{comp,hf}}{C_{comp,lf} + C_{comp,hf}}}. \tag{3.35}$$
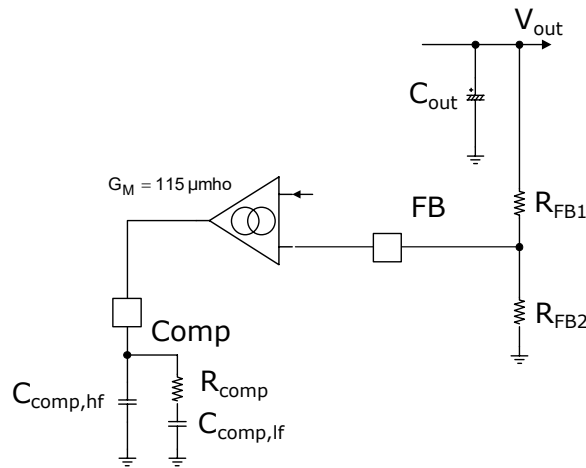
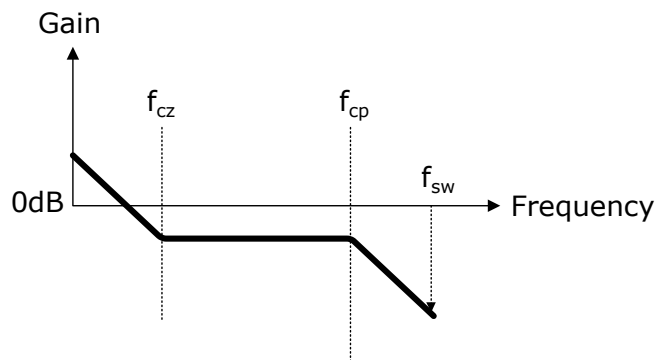**Figure 3.10.** Boost converter feedback circuit.

Figure 3.11. Boost converter compensation network gain plot.

If the low frequency compensation capacitor, $C_{comp,lf}$ is much larger than the high-frequency compensation capacitor, $C_{comp,hf}$, then f_I and f_{cp} can be simplified to (3.36) and (3.37).

$$f_I = \frac{2.5}{V_{out}} \cdot \frac{115\mu mho}{2\pi \cdot C_{comp,lf}} \tag{3.36}$$

$$f_{cp} = \frac{1}{2\pi \cdot R_{comp} \cdot C_{comp,hf}} \tag{3.37}$$

Figure 3.10 show the feedback network of the boost converter. Figure 3.11 show the gain plotted against frequency for the compensation network. The compensation zero, as well as the compensation pole, is also indicated on the graph.

The component values of the compensation network are calculated by determining the crossover frequency that is about 0.1 to 0.2 of the line frequency. The power stage control to output transfer function has a -20 $dB/decade$ slope and a -90° phase at the crossover frequency. This can be seen
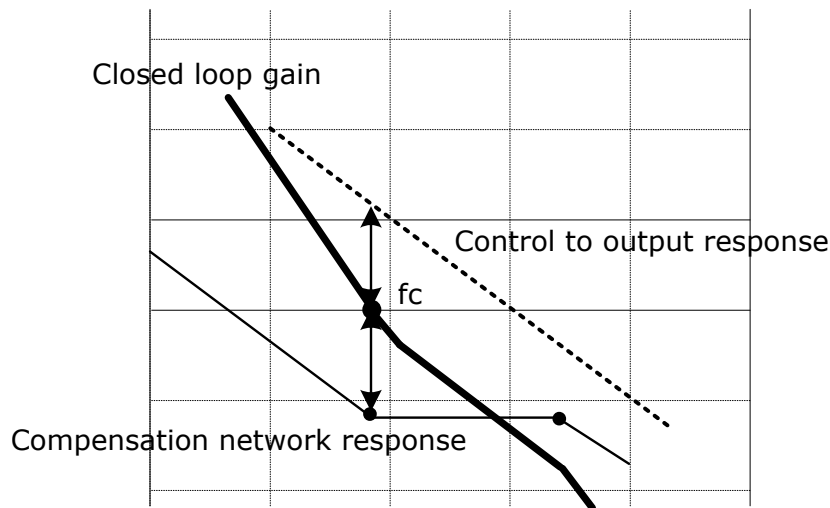
Figure 3.12. Boost converter compensation network gain plot.

in Figure 3.12. The compensation zero should be placed at the crossover frequency in order to obtain a 45° phase margin. The zero compensation capacitor, $C_{comp,zero}$, is given by (3.38) and the compensation resistor, R_{comp}, for the zero at the crossover frequency is given by (3.41) The high frequency compensation pole should be placed at least a decade higher than the crossover frequency in order to ensure that the pole does not interfere with the phase margin of the voltage regulation loop at the crossover frequency. The pole frequency should also be lower than the switching frequency to ensure that noise is effectively attenuated. The pole compensation capacitor, $C_{comp,pole}$, is given by (3.44). The component values can be calculated by choosing the crossover frequency, f_c, and thus also the control bandwidth at 15 Hz and the high-frequency pole, f_{cp} at 120 Hz.

$$C_{comp,zero} = \frac{K_{SAW} \cdot V_{Line}^2 \cdot 2.5 \cdot 115\mu mho}{2 \cdot V_{out}^2 \cdot L \cdot C_{out} \cdot (2\pi f_c)^2} \tag{3.38}$$

$$= \frac{8.50x10^{-6} \cdot 240^2 \cdot 2.5 \cdot 115\mu mho}{2 \cdot 440^2 \cdot 1.5x10^{-3} \cdot 4x10^{-6} \cdot (2\pi 15)^2} \tag{3.39}$$

$$= 6.8 \ \mu F \tag{3.40}$$

Choose $C_{comp,zero}$ to be 5 µF.

$$R_{comp} = \frac{1}{2\pi \cdot f_c \cdot C_{comp,zero}} \tag{3.41}$$

$$= \frac{1}{2\pi \cdot 15 \cdot 5x10^{-6}} \tag{3.42}$$

$$= 2.122 \ k\Omega \tag{3.43}$$

Choose $R_{comp} = 2$ kΩ.

$$C_{comp,pole} = \frac{1}{2\pi \cdot f_{cp} \cdot R_{comp}} \tag{3.44}$$

$$= \frac{1}{2\pi \cdot 120 \cdot 2x10^3} \tag{3.45}$$

$$= 663.1 \text{ nF} \tag{3.46}$$

Choose $C_{comp,pole}$ to be 680 nF.

The feedback voltage as well as the over and under voltage protection voltages are set by resistors that were calculated by the following equations. The output voltage V_{out} and maximum output voltage $V_{out,max}$ is defined in (3.47) and (3.48), respectively. The values for these voltages were set using a series of resistors, R_{out1}, R_{out2} and R_{out3}. The value of R_{out2} was chosen since there were only two equations but three variables. The under voltage protection $V_{out(UV)}$ was calculated using (3.49). The reference voltage V_{ref} was obtained from the datasheet. R_{out2} was chosen to be 24 kΩ, while R_{out1} was calculated as 3.96 MΩ and R_{out3} was calculated as 900 Ω.

$$V_{out} = \frac{R_{out1} + R_{out2} + R_{out3}}{R_{out2} + R_{out3}} V_{ref} \tag{3.47}$$

$$V_{out,max} = \frac{R_{out1} + R_{out2} + R_{out3}}{R_{out2}} V_{ref} \tag{3.48}$$

$$V_{out(UV)} = 0.12V_{out,max} \tag{3.49}$$

$$= 0.12 \cdot 440 \tag{3.50}$$

$$= 52.8 \text{ V} \tag{3.51}$$

The capacitance of the on-time capacitor C_t was calculated using (3.52). The internal reference voltage V_{ref} was obtained from the datasheet. An offset had to be applied to the on-time especially at high line voltage inputs while the device is under a low load. To do this, two resistors were added to the circuit, namely R_{offset} and R_{drv2} to ensure that the offset is large enough. These resistors should form a 400 mV to 500 mV offset when the switch is on. In order to achieve the same on time, the on-time capacitor was adjusted. This is shown in (3.55). To ensure that the follower booster function is turned

off, a higher capacitor value was chosen.

$$C_t = \frac{120 \cdot 10^{-6} V_{ref}^2 L P_{out}}{\eta \left(V_{ac,min}\right)^2} \tag{3.52}$$

$$= \frac{120 \cdot 10^{-6} \cdot 2.5^2 \cdot 1.5 \cdot 10^{-3} \cdot 30}{0.93 \cdot 88^2} \tag{3.53}$$

$$= 4.69 \text{ nF} \tag{3.54}$$

R_{offset} was calculated as 56 kΩ and R_{drv2} was calculated as 4.7 kΩ

$$C_{t,offset} = \frac{C_{t,nom}}{1 - V_{offset}} \tag{3.55}$$

$$= \frac{4.69 \cdot 10^{-9}}{1 - 0.18} \tag{3.56}$$

$$= 5.71 \text{ nF} \tag{3.57}$$

$C_{t,offset}$ was calculated as 10 nF

The MOSFET is designed by using the peak voltage stress and RMS current stress. The RMS current through the MOSFET $I_{M,RMS}$ was calculated using (3.58). The MOSFET should also have a low drain capacitance since this capacitance will be charged and discharged every switching cycle. Switching losses can thus be reduced and the efficiency increased by keeping the grain capacitance as low as possible. It is also important to keep the on state drain to source resistance low when the MOSFET is switched on to minimise the conduction losses without increasing the switching losses to much.

$$I_{M,RMS} = \frac{2P_{out}}{\sqrt{3}\eta V_{ac,min}} \sqrt{1 - \frac{8\sqrt{2}V_{ac,min}}{3\pi V_{out}}} \tag{3.58}$$

$$= \frac{2 \cdot 30}{\sqrt{3} \cdot 0.93 \cdot 88} \sqrt{1 - \frac{8 \cdot \sqrt{2} \cdot 88}{3\pi 430}} \tag{3.59}$$

$$= 0.36 \text{ A} \tag{3.60}$$

The conduction losses of the MOSFET P_{cond} was calculated in (3.61). It was also assumed that $R_{ds(on)}$ will increase by 80% due to temperature effects.

$$P_{cond} = I_{M,RMS}^2 R_{ds(on)} \tag{3.61}$$

$$= 0.36^2 \cdot 0.19 \cdot 1.8 \tag{3.62}$$

$$= 0.04 \text{ W} \tag{3.63}$$

Selecting the boost diode was simple since there are no reverse recovery times to take into account. This is due to the fact that the critical conduction mode is used and the current through the inductor and diode is zero when it switches off. The peak current through the diode is the same as that through the boost inductor. The voltage over the diode is the same as the output voltage plus a safety margin to protect the diode.

Output voltage ripple caused by the equivalent series resistance (ESR) of the output capacitor should not be a big problem since the output voltage is high and the load current low. The output voltage ripple should, however, be kept low enough to prevent the controller from detecting an over voltage event and going into the over voltage protection mode. The voltage ripple of the output capacitor was calculated using (3.64). The current ripple of the output capacitor was calculated using (3.67) and the hold-up time is given by (3.70).

$$V_{ripple(p-p)} = \frac{P_{out}}{2\pi f_{line} C_{out} V_{out}} \tag{3.64}$$

$$16 = \frac{50}{2\pi \cdot 50 \cdot C_{out} \cdot 430} \tag{3.65}$$

$$C_{out} = 23.87 \ \mu\text{F} \tag{3.66}$$

$$I_{Cout,RMS} = \sqrt{\frac{32\sqrt{2}P_{out}^2}{\pi V_{ac,min} V_{out} \eta^2} - \left(\frac{P_{out}}{V_{out}}\right)^2} \tag{3.67}$$

$$= \sqrt{\frac{32\sqrt{2} \cdot 50^2}{\pi \cdot 88 \cdot 430 \cdot 0.93^2} - \left(\frac{30}{430}\right)^2} \tag{3.68}$$

$$= 0.20 \ \text{A} \tag{3.69}$$

$$t_{holdup} = \frac{C_{out}\left(V_{out}^2 - V_{min}^2\right)}{2P_{out}} \tag{3.70}$$

$$16 \cdot 10^{-3} = \frac{C_{out}\left(430^2 - 380^2\right)}{2 \cdot 50} \tag{3.71}$$

$$C_{out} = 3.95 \ \mu\text{F} \tag{3.72}$$

The output capacitor thus had to have a capacitance of at least 4 μF to comply with the requirements.

The circuit for the boost converter module is shown in Figure 3.13 and the PCB layout in Figure 3.14. The input voltage is connected to P3 after which it is rectified. The current flow from the bridge rectifier through the boost inductor and the also through the output diode to the output capacitor. The

output voltage is then supplied on the P4 header. The controller with all of the relevant control signal circuitry is placed below the main current path of the boost converter.

3.4 ELECTROMAGNETIC INTERFERENCE MODULE DESIGN AND AUXILIARY POWER SUPPLY DESIGN CONSIDERATIONS

3.4.1 EMI Design Equations

An EMI filter is necessary to ensure that switching noise is not conducted to the mains power lines and to ensure that any noise on the mains power lines is filtered out. An iterative method was used to determine all of the circuit parameters since there are too many unknowns in the circuit and the conducted EMI on the power lines was also unknown. The common mode inductor L_C value was calculated using (3.73). The value of the Y capacitor C_Y was chosen to be 3300 pF and the common mode corner frequency is 20 kHz.

$$L_C = \left(\frac{1}{2\pi f_{CM}}\right)^2 \cdot \frac{1}{2C_Y} \tag{3.73}$$

$$= \left(\frac{1}{2 \cdot \pi \cdot 20 \cdot 10^3}\right)^2 \cdot \frac{1}{2 \cdot 3300 \cdot 10^{-12}} \tag{3.74}$$

$$= 9.6 \text{ mH} \tag{3.75}$$

The differential mode inductor L_D value was calculated using (3.76). The value of the X capacitor C_X was chosen to be 0.47 μF and the differential mode corner frequency is 10 kHz.

$$L_D = \left(\frac{1}{2\pi f_{DM}}\right)^2 \cdot \frac{1}{2C_X} \tag{3.76}$$

$$= \left(\frac{1}{2 \cdot \pi \cdot 10 \cdot 10^3}\right)^2 \cdot \frac{1}{0.47 \cdot 10^{-6}} \tag{3.77}$$

$$= 540 \text{ μH} \tag{3.78}$$

3.4.2 Auxiliary power supply design considerations

An auxiliary power supply was needed to supply power to the boost controller. To ensure that this power supply was as compact and efficient as possible another self-driving boost switch-mode controller was selected. This controller is capable of supplying 8 W of output power at 15 V. Large heat sinks or active
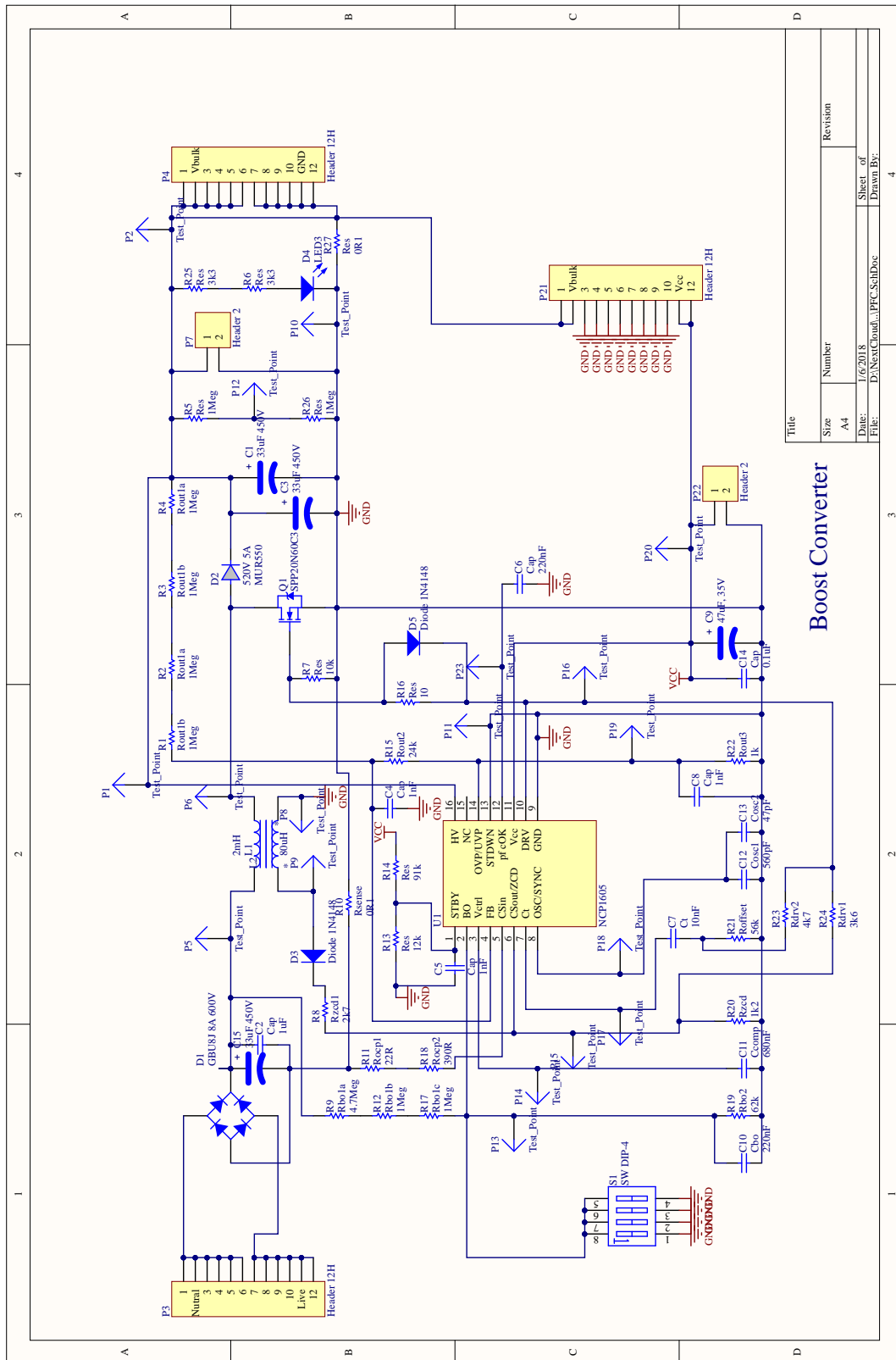
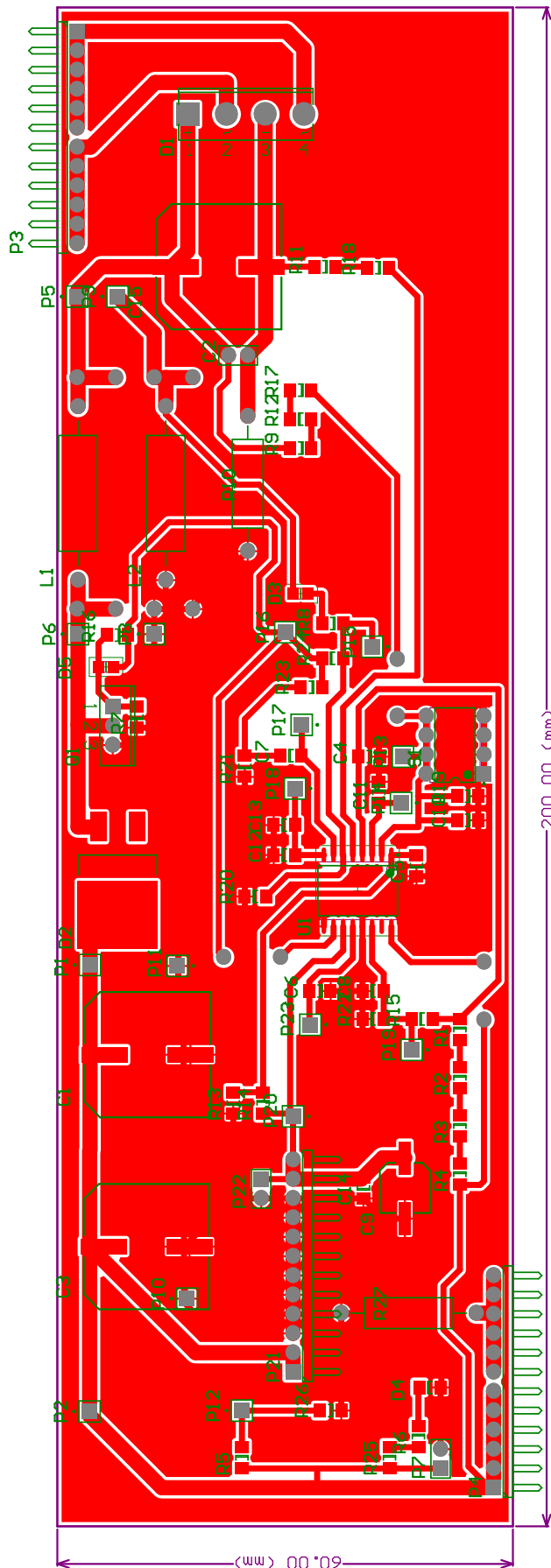**Figure 3.13.** Boost converter module schematic.

Figure 3.14. Boost converter module printed circuit board (PCB) layout.

cooling for the auxiliary power supply were unnecessary since this module was efficient. By using an auxiliary power supply to supply power to the boost controller of the primary power supply, meant that the boost inductor could be made significantly smaller since there is no need for auxiliary windings. The standby and on-line power consumption of the primary boost converter were also decreased by the use of the efficient low power auxiliary power supply, resulting in an overall efficient design.

3.5   CHAPTER CONCLUSION

The component values of the boost converter and EMI filter were calculated in this chapter to ensure that the required output response could be obtained and that the power supply would be stable over the operating frequency. The design considerations for the auxiliary power supply were also discussed to ensure that this power supply could be designed to meet the necessary output requirements.

CHAPTER 4   SPEAKER MODEL DESIGN

4.1   MODEL CALCULATIONS FOR A SINGLE SPEAKER

The speaker cabinet simulation model was developed by using the Thiele-Small parameters for the speaker and the dimensions of the cabinet [26]. The Thiele-Small parameters for a single speaker in a closed cabinet are shown in Table 4.1 and that of a closed cabinet with two parallel connected speakers in Table 4.2. The simulation model, shown in Figure 4.1, was constructed by combining the models for the electrical, mechanical and acoustical speaker parts into one simulation model to gain an accurate representation of the speaker and cabinet.

The compliance of the speaker diaphragm assembly is modelled by L_{ces}, the mass of the diaphragm by C_{mes}, and the mechanical damping of the diaphragm assembly R_{es} [26]. These three parameters represent the mechanical characteristics of the speaker driver or the voice coil. The electrical characteristics of the driver are represented by electrical self-inductance L_e and DC resistance R_e [26]. Because the speaker is installed in an enclosure, the acoustical load on both sides of the speaker will differ. This acoustical component is modelled by L_{ceb} because the cabinet acts as a spring on the speaker diaphragm [26]. The Thiele-Small parameters were used to calculate the component values for the mechanical components by solving Equations 4.1 to 4.3. The mechanical quality factor is given by Q_{MS}, the electrical quality factor by Q_{ES} and the resonance frequency by f_s in the equations below.

$$Q_{ES} = 2\pi f_s C_{mes} R_e \tag{4.1}$$

$$Q_{MS} = 2\pi f_s C_{mes} R_{es} \tag{4.2}$$

$$f_s = \frac{1}{2\pi\sqrt{C_{mes}L_{ces}}} \tag{4.3}$$

Table 4.1. Thiele-Small parameters for one speaker in a closed cabinet.

Symbol	Parameter
R_e	DC resistance of voice coil
L_e	Self-inductance of voice coil
Bl	Force factor
M_{MD}	Mass of diaphragm
C_{MS}	Compliance of suspension
R_{MS}	Mechanical damping
f_S	Resonance frequency
Q_{MS}	Mechanical quality factor
Q_{ES}	Electrical quality factor
Q_{TS}	Total quality factor
SD	Area of diaphragm
V_{AS}	Equivalent volume
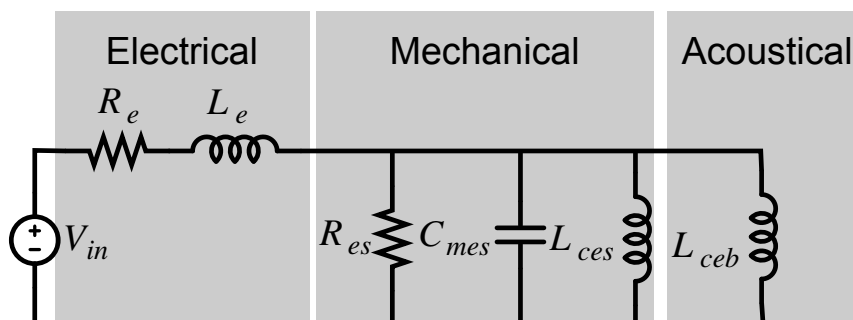
Figure 4.1. Generic speaker and cabinet simulation model.

The enclosure introduces a new compliance ratio parameter, α, which is the ratio between the equivalent and enclosure volumes. This parameter corresponds to the ratio between the mechanical and acoustical compliance inductor values [26]. The acoustical inductor value was calculated by solving Equation 4.4.

$$\alpha = \frac{V_{AS}}{V_{AB}} = \frac{L_{ces}}{L_{ceb}} \tag{4.4}$$

The volume compliance ratio shifted the resonance frequency and quality factor of the speaker and cabinet system [26]. The shifted resonance frequency f_c and quality factor Q_{TC} were calculated by

Table 4.2. Thiele-Small parameters for two speakers in a closed cabinet.

Symbol	Parameter
$R_e/2$	DC resistance of voice coil
$L_e/2$	Self-inductance of voice coil
Bl	Force factor
M_{MD}	Mass of diaphragm
C_{MS}	Compliance of suspension
R_{MS}	Mechanical damping
f_S	Resonance frequency
Q_{MS}	Mechanical quality factor
Q_{ES}	Electrical quality factor
Q_{TS}	Total quality factor
$2SD$	Area of diaphragm
$2V_{AS}$	Equivalent volume

solving Equations 4.5 and 4.6.

$$f_c \approx f_s\sqrt{1+\alpha} \tag{4.5}$$

$$Q_{TC} \approx Q_{TS}\sqrt{1+\alpha} \tag{4.6}$$

To calculate the 3 dB cut-off frequency of the speaker cabinet system, Equation 4.7 was solved [26].

$$f_t = f_c \left[\left(\frac{1}{2Q_{TC}^2} - 1 \right) + \sqrt{\left(\frac{1}{2Q_{TC}^2} - 1 \right)^2 + 1} \right]^{1/2} \tag{4.7}$$

The speaker cabinet model is shown in Figure 4.2, with all of the relevant parameters. The calculations for a closed cabinet with two parallel connected speakers are shown in the next subsection. The parameters for a single speaker model in a closed cabinet are shown in Table 4.3 and that of a closed cabinet with two speakers connected in parallel in Table 4.4.
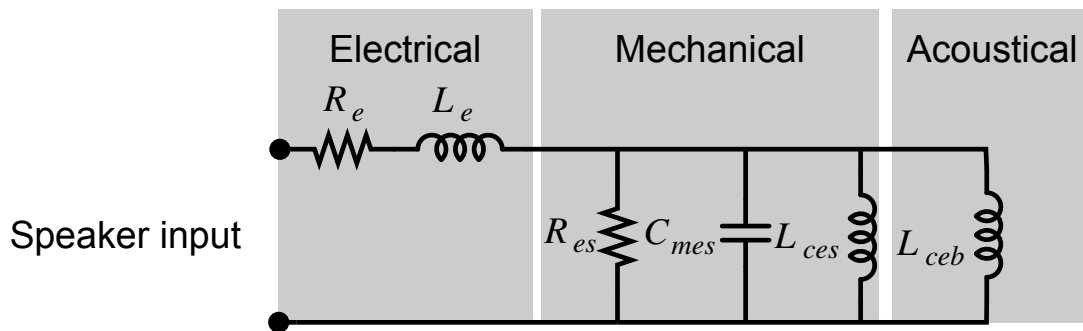
Figure 4.2. Speaker and cabinet simulation model.

4.2 MODEL CALCULATIONS FOR TWO PARALLEL CONNECTED SPEAKERS

The Thiele-Small speaker parameters are shown in Table 4.5.

The component values of the speaker model were calculated, using Equations 4.8 to 4.17. The model was then constructed and used to test the amplifier to eliminate excessive noise while testing the amplifier near its power limit, thus in the saturation region. The new resonant frequency of the speaker and enclosure is given by Equation 4.21 and the new quality factor is given by Equation 4.24. The speaker model is shown in Figure 4.2.

$$Q_{ES} = 2\pi f_s C_{mes} R_E \tag{4.8}$$

$$9.53 = 2 \cdot \pi \cdot 89 \cdot C_{mes} \cdot 6.03 \tag{4.9}$$

$$C_{mes} = 2.83 \text{ mF} \tag{4.10}$$

$$Q_{MS} = 2\pi f_s C_{mes} R_{es} \tag{4.11}$$

$$16.33 = 2 \cdot \pi \cdot 89 \cdot 0.00282 \cdot R_{es} \tag{4.12}$$

$$R_{es} = 10.33 \ \Omega \tag{4.13}$$

$$f_s = \frac{1}{2\pi\sqrt{C_{mes}L_{ces}}} \tag{4.14}$$

$$89 = \frac{1}{2\pi\sqrt{0.00282 \cdot L_{ces}}} \tag{4.15}$$

$$L_{ces} = 1.13 \text{ mH} \tag{4.16}$$

Table 4.3. Speaker model parameters for a single speaker.

Parameter	Value
R_e	12.06 Ω
L_e	0.76 mH
f_s	89 Hz
Q_{MS}	16.33
Q_{ES}	9.53
Q_{TS}	6.02
C_{mes}	1.41 mF
L_{ces}	2.267 mH
L_{ceb}	4.617 mH
R_{es}	20.665 Ω
l	6.15 mm
B	2.65 T
H	5.15 A/m
f_c	108.67 Hz

$$\alpha = \frac{V_{AS}}{V_{AB}} = \frac{L_{ces}}{L_{ceb}} \tag{4.17}$$

$$\frac{82.42}{6.15 \cdot 2.65 \cdot 5.15} = \frac{0.00113}{L_{ceb}} \tag{4.18}$$

$$\frac{82.42}{83.932} = \frac{0.00113}{L_{ceb}} \tag{4.19}$$

$$L_{ceb} = 1.15 \text{ mH} \tag{4.20}$$

$$f_c \approx f_s\sqrt{1+\alpha} \tag{4.21}$$

$$f_c \approx 89\sqrt{1+0.982} \tag{4.22}$$

$$f_c \approx 125.30 \text{ Hz} \tag{4.23}$$

$$Q_{TC} \approx Q_{TS}\sqrt{1+\alpha} \tag{4.24}$$

$$Q_{TC} \approx 6.02\sqrt{1+0.982} \tag{4.25}$$

$$Q_{TC} \approx 8.48 \tag{4.26}$$

Table 4.4. Speaker model parameters for two speakers connected in parallel.

Parameter	Value
R_e	6.03 Ω
L_e	0.38 mH
f_s	89 Hz
Q_{MS}	16.33
Q_{ES}	9.53
Q_{TS}	6.02
C_{mes}	2.83 mF
L_{ces}	1.13 mH
L_{ceb}	1.15 mH
R_{es}	10.33 Ω
l	6.15 mm
B	2.65 T
H	5.15 A/m
f_c	125.30 Hz

4.3   CHAPTER CONCLUSION

The speaker model component values for two parallel connected speakers in a closed speaker cabinet were calculated in this chapter. This was done to eliminate the noise generated by testing the amplifier at high volume and ensured that repeatable results could be obtained from the amplifier.

Table 4.5. Thiele-Small parameters for closed cabinet with two parallel connected speakers.

Parameter	Value
Resonant Frequency (f_s)	89 Hz
DC Resistance (R_e)	6.03 Ω
Coil Inductance (L_e)	0.38 mH
Mechanical Q (Q_{ms})	16.33
Electromagnetic Q (Q_{es})	9.53
Total Q (Q_{ts})	6.02
Compliance Equivalent Volume (V_{as})	82.42 l
Peak Diaphragm Displacement Volume (V_d)	24.42 cc
Mechanical Compliance of Suspension (C_{ms})	0.11 mm/N
Bl Product (Bl)	4.48 T-m
Diaphragm Mass Inc. Air load (MMs)	28.3 g
Efficiency Bandwidth Product (EBP)	9.34 Hz
Maximum Linear Excursion (X_{max})	0.047 mm
Surface Area of Cone (S_d)	1036 cm^2
Maximum Mechanical Limit (X_{lim})	N/A

CHAPTER 5   RESULTS

5.1   CHAPTER OVERVIEW

The results of the study are discussed in this section. The amplifier was first simulated in order to obtain a simulation model to test the switch-mode power supply design. The amplifier was then tested and the results were used to verify that the simulation model is accurate. These test results were also used to validate the results obtained when the amplifier was tested while powered by the switch-mode power supply. The latter was then constructed and the amplifier was tested while being powered by the switch-mode power supply. These results were then compared to the measurements obtained from the amplifier while powered by the unregulated power supply.

5.2   OUTPUT IMPEDANCE CALCULATIONS

The output impedance of the power supplies was calculated by using the averaging and linearisation procedure. The output impedance of the power supplies was calculated by applying a test input current at the output of the power supply and then calculating the output voltage response to the test current. The open loop output impedance could then be calculated when the output voltage and current were known. The open loop output impedance of the unregulated as well as the switch-mode power supplies are calculated below.

5.2.1   Output impedance calculation of the unregulated power supply

From Figure 5.1 the output impedance of the unregulated power supply can be calculated. By applying Kirchhoff's current law to the output nodes (5.1) was obtained. By taking (5.2) into account, noting that
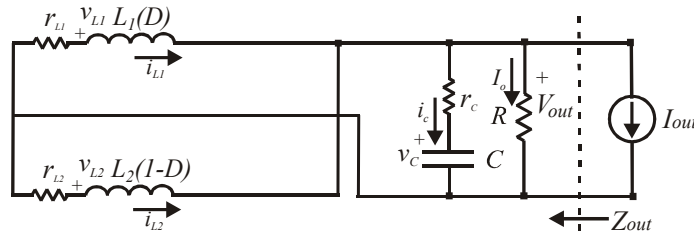
Figure 5.1. Unregulated power supply small-signal model to calculate the output impedance.

i_{L1} is equal to i_{L2} since it is a centre tapped transformer, that the duty cycle D is 50% and substituting (5.1) into (5.2), the output impedance is given by (5.3). The output impedance was then calculated by substituting $s = j\omega$ and then $\omega = 2\pi f$, where $f = 100\ Hz$ into the equation.

$$i_{L2}(1-D) + i_{L1}(D) = \frac{V_{out}}{r_c + \frac{1}{sC}} + \frac{V_{out}}{R} + I_{out} \tag{5.1}$$

$$i_L = \frac{V_{out}}{sL + r_L} \tag{5.2}$$

$$Z_{out} = \frac{V_{out}(s)}{I_{out}(s)} = \frac{R(sCr_c + 1)(sL + r_L)}{-s^2 LC(R + r_c) - s[L - RCr_c + Cr_L(R + r_c)] + R - r_L} \tag{5.3}$$

$$= \frac{220 \times 10^3 (s \cdot 16 \times 10^{-6} \cdot 12.5 + 1)(s \cdot 1.6 \times 10^{-3} + 35.4)}{\begin{array}{c} -s^2 \cdot 1.6 \times 10^{-3} \cdot 16 \times 10^{-6}(220 \times 10^3 + 12.5) - s[1.6 \times 10^{-3} - 220 \times 10^3 \cdot 16 \times 10^{-6} \cdot 12.5 \\ + 16 \times 10^{-6} \cdot 35.4(220 \times 10^3 + 12.5)] + 220 \times 10^3 - 35.4 \end{array}}$$

$$\tag{5.4}$$

$$= 30.98 - 9.56j \tag{5.5}$$

$$= 32.41 e^{-0.30j} \tag{5.6}$$

5.2.2 Output impedance calculation of the switch-mode power supply

From Figure 5.2 the output impedance of the boost converter can be calculated. By applying Kirchhoff's current law to the output nodes and by setting the supply, V_s, to zero, (5.7) was obtained. By taking (5.8) into account and substituting (5.7) into (5.8), the output impedance is given by (5.9). The output impedance was then calculated by substituting $s = j\omega$ and then $\omega = 2\pi f$, where $f = 80\ kHz$ and $D = 0.49$ into the equation.

$$i_L(1-D) = \frac{V_{out}}{r_c + \frac{1}{sC}} + \frac{V_{out}}{R} + I_{out} \tag{5.7}$$

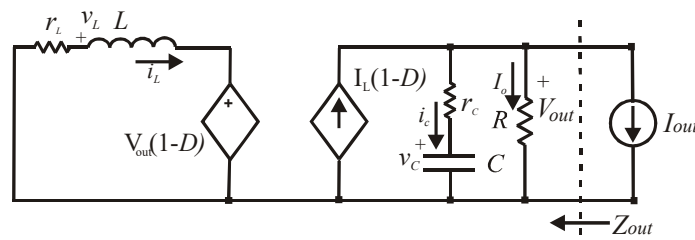$$i_L = \frac{V_{out}(1-D)}{sL + r_L} \tag{5.8}$$

Figure 5.2. Boost converter small-signal model to calculate the output impedance.

$$Z_{out} = \frac{V_{out}(s)}{I_{out}(s)} = \frac{R(sCr_c + 1)(sL + r_L)}{-s^2 LC(R + r_c) - s[L - RCr_c(1 - D)^2 + Cr_L(R + r_c)] + R(1 - D)^2 - r_L} \tag{5.9}$$

$$= \frac{220 \times 10^3 (s \cdot 4 \times 10^{-6} \cdot 12.5 + 1)(s \cdot 1.5 \times 10^{-3} + 1.2)}{\begin{array}{c} -s^2 \cdot 1.5 \times 10^{-3} \cdot 4 \times 10^{-6}(220 \times 10^3 + 12.5) - s[1.5 \times 10^{-3} - 220 \times 10^3 \cdot s \cdot 4 \times 10^{-6} \cdot \\ 12.5(1 - D)^2 + 4 \times 10^{-6} \cdot 1.2(220 \times 10^3 + 12.5)] + 220 \times 10^3 (1 - D)^2 - 1.2 \end{array}}$$
$$\tag{5.10}$$

$$= 12.50 - 0.40j \tag{5.11}$$

$$= 12.51 e^{-0.03j} \tag{5.12}$$

5.3   FENDER DELUXE 5E3 SIMULATION MODEL MEASUREMENTS

The Fender Deluxe 5E3 simulation model is shown in Figure 5.3. The guitar input is connected to either the normal or bright input of the amplifier where the signal is amplified by the first pre-amplification stage. Following the first amplification stage is the tone stack of the amplifier where the volume of each of the two input channels can be adjusted as well as the tone of the audio signal. The signal is then amplified by the second pre-amplification stage. The signal from the second pre-amplifier stage is then fed to the phase splitter, or phase inverter, where a second signal that is 180 ° out of phase with the input signal is generated. These two signals are then fed to the class AB push-pull power amplification stage where the audio signal is amplified one last time in order to drive the high voltage audio transformer. The secondary side of the audio transformer is connected to the speaker. The power supply is used to supply high voltage power to the pre-amplifier, power amplifier and central tap of the audio transformer. This model was used to test the effects of the power supply on the amplifier, as well as to test the switch-mode power supply simulation model to ensure that additional noise was not added to the output of the amplifier. The measurements in Table 5.1 were taken to ensure that the power supply and bias voltages could be compared to that of the amplifier measurements in the sections below.
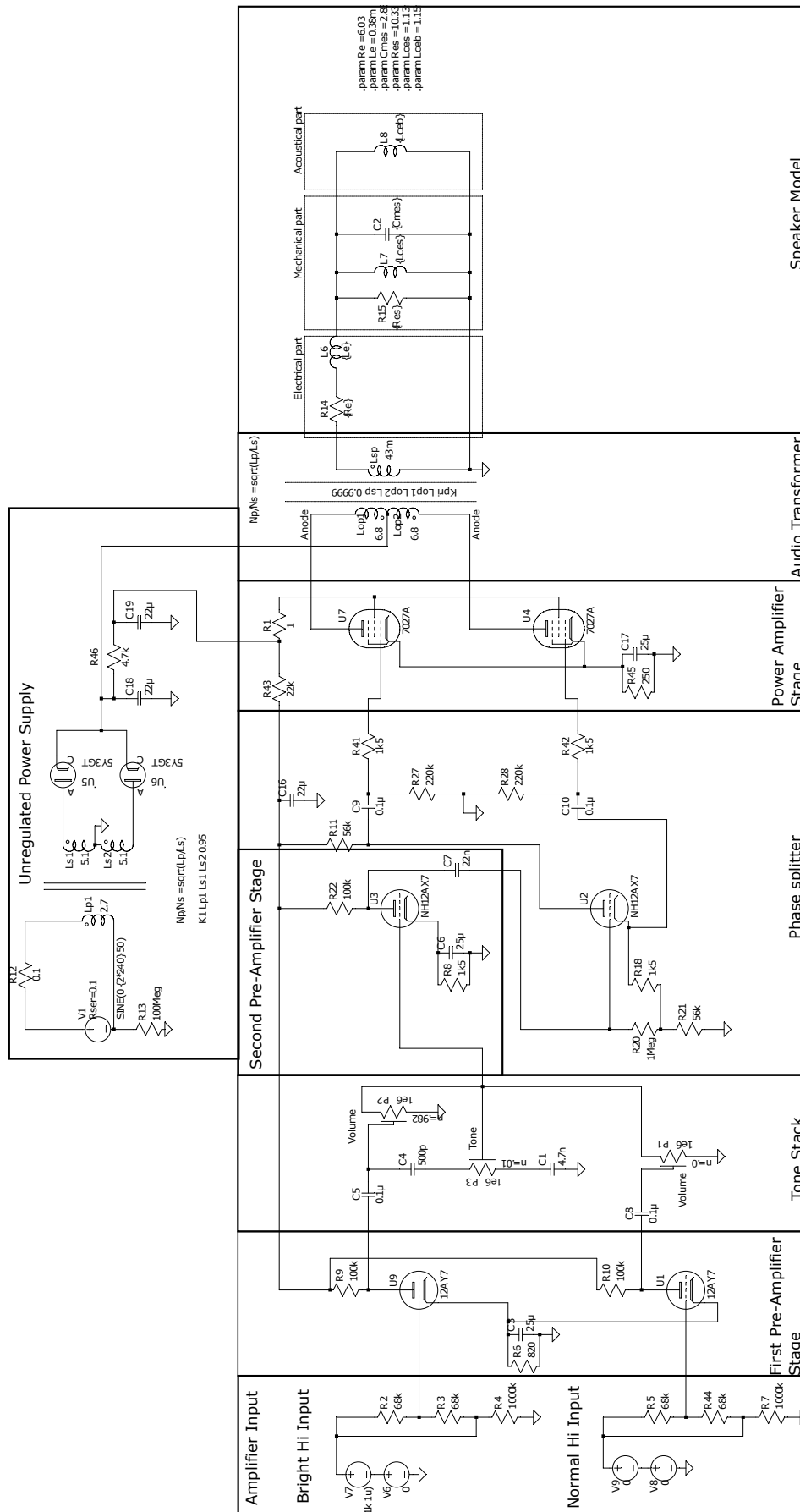
Figure 5.3. Fender Deluxe 5E3 simulation model.

Table 5.1. Voltage measurements of the amplifier model.

Parameter	Value
High voltage on the output transformer	430 V
Plate voltage on output tube 1	422 V
Plate voltage on output tube 2	422 V
High voltage for output tube screens	375 V
High voltage for pre-amplifier tube plates	278 V
Voltage over output tube biasing resistor	30.4 V
Voltage over 12AY7 tube biasing resistor	2.28 V
Voltage over 12AX7 tube biasing resistor	1. 47 V

The AC component of the output steady-state simulation results of the Fender Deluxe 5E3 power supply section are shown in Figure 5.4. The transient response of the unregulated power supply simulation is shown in Figure 5.5. From these simulations, it can be concluded that the power supply output is not regulated since the output of the high voltage supply suddenly lower when a load is connected and then recovers when the load is disconnected without any overshoot. The high voltage supplied to the power amplifier and pre-amplifier stages had less voltage ripple and were thus more stable and will have a very small effect on the output signal of the amplifier. From the results in Figure 5.4 and Figure 5.5, it can be concluded that the high voltage output supplying the output transformer had the largest influence on the output response of the amplifier and the high voltage supply to the power stage had the second biggest influence. This is because the output voltage from the audio transformer and thus also the voltage over the speakers are directly proportional to that of the centre tapped input of the transformer and can change rapidly with varying current demands.

The Fender deluxe 5E3 simulation model output steady-state response is shown in Figure 5.6. No distortion is visible on the outputs of the amplifier as it was not driven at high enough power levels to induce saturation and distortion in the power amplifier section. There is AC hum visible on the output of the power supply which has a very small effect on the output signal of the amplifier.

The Fender Deluxe 5E3 frequency response is shown in Figure 5.7 indicating that it has a bandwidth of 16.6 kHz. This confirms that the bandwidth is within the human audible range and that the amplifier will act as a low pass filter. From this, it can be deduced that the high-frequency switching noise of the
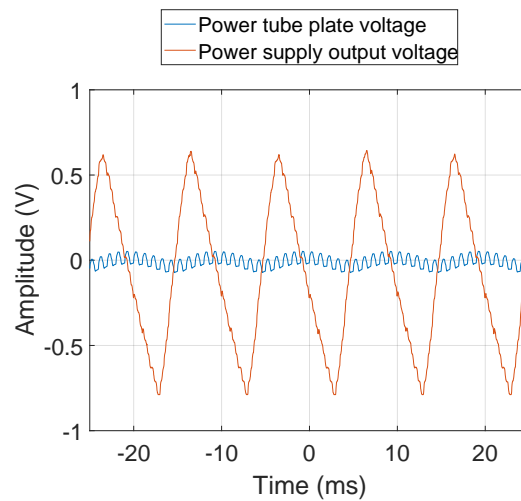
Figure 5.4. Fender Deluxe 5E3 power supply steady-state response.
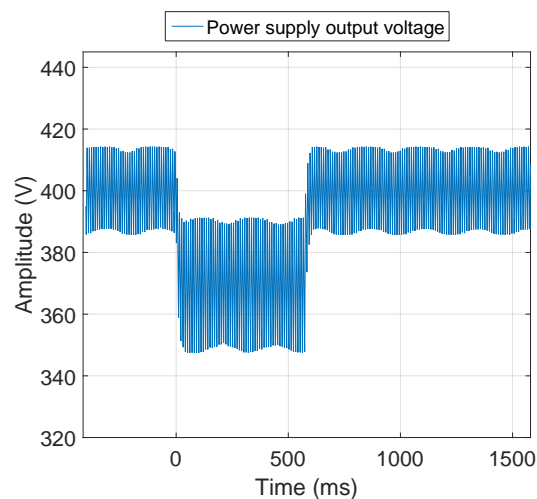

Figure 5.5. Fender Deluxe 5E3 simulation model unregulated power supply transient response.

switch-mode power supply will be suppressed by the amplifier as long as the frequency is outside the bandwidth of the amplifier. This result was used to compare the frequency response of the simulation model to that of the amplifier to ensure that the models were accurate.

The output distortion of the Fender Deluxe 5E3 simulation model can be seen in Figure 5.8. This figure compares the sinusoidal input signal of 1 kHz of the amplifier to the output signal to determine the total harmonic distortion (THD) at high volume levels. The THD is calculated as 12%.
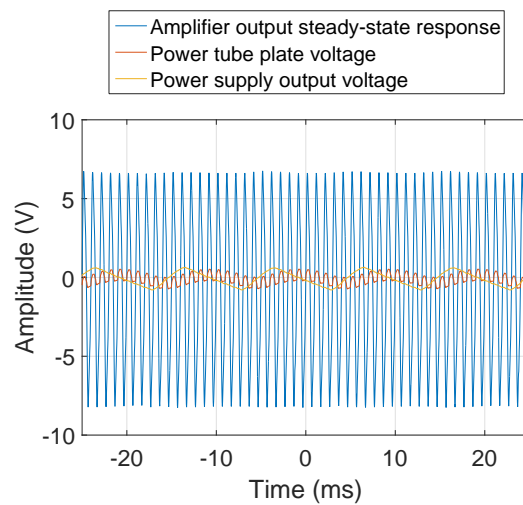
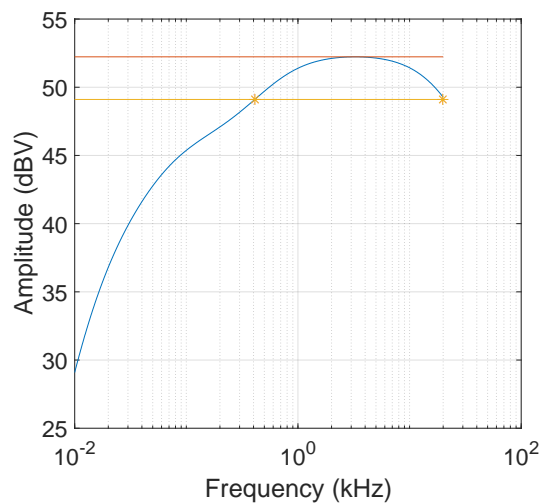**Figure 5.6.** Fender Deluxe 5E3 output steady-state response.

Figure 5.7. Fender Deluxe 5E3 output frequency response.

5.4   FENDER DELUXE 5E3 PRACTICAL MEASUREMENTS

5.4.1   Measurements with the unregulated power supply

The Fender Deluxe 5E3 amplifier, with its unregulated power supply, was constructed and tested to obtain data to compare to the results obtained while it was powered by the switch-mode power supply. These measurements were also used to confirm that the simulation model was accurate. The
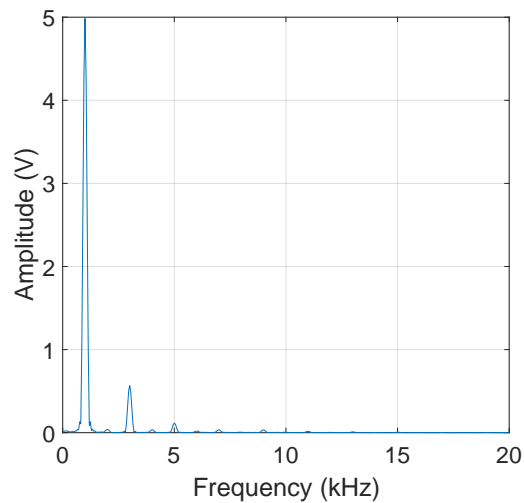
Figure 5.8. Fender Deluxe 5E3 output distortion of a 1 kHz sine wave.

Table 5.2. Voltage measurements of the amplifier when powered by the unregulated power supply.

Parameter	Value
High voltage on the output transformer	429.8 V
Plate voltage on output tube 1	419.6 V
Plate voltage on output tube 2	419.8 V
High voltage for output tube screens	386.6 V
High voltage for pre-amplifier tube plates	278.3 V
Voltage over output tube biasing resistor	27.9 V
Voltage over 12AY7 tube biasing resistor	2.25 V
Voltage over 12AX7 tube biasing resistor	1.41 V

measurements in Table 5.2 were taken to ensure that the power supply voltages and bias voltages could be compared to that of the amplifier while powered by the switch-mode power supply.

The AC component of the output steady-state response results of the Fender Deluxe 5E3 unregulated power supply section are shown in Figure 5.9. The transient response of the switch-mode power supply is shown in Figure 5.16. From these graphs, it is clear that the power supply output is not regulated since the high voltage output of the power supply do not compensate in any way when a load is connected to the output of the power supply. The output voltage only drops when the load is
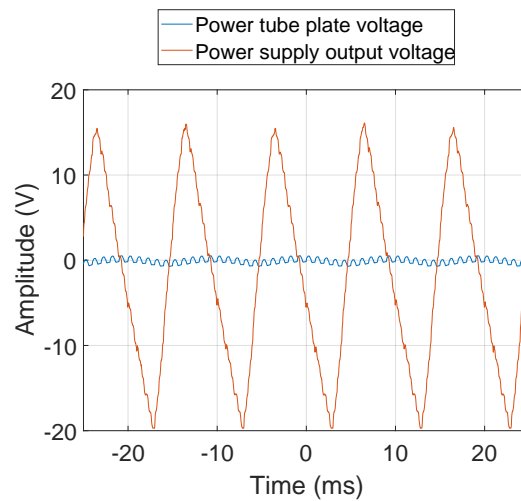
Figure 5.9. Fender Deluxe 5E3 unregulated power supply steady-state response.
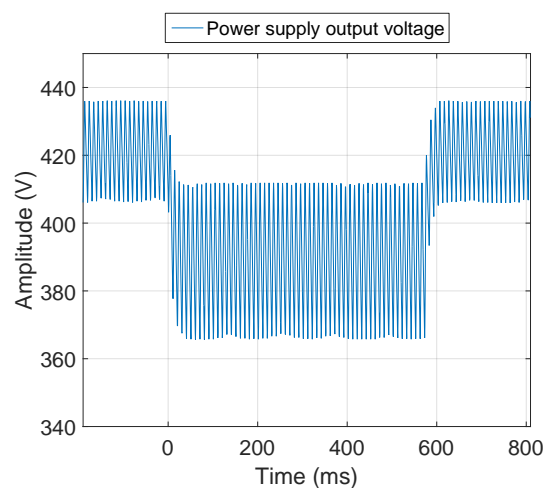

Figure 5.10. Fender Deluxe 5E3 unregulated power supply transient response.

connected and then recovers when the load is disconnected without any over or undershoot. The high voltage supplied to the power amplifier and pre-amplifier stages had less output voltage ripple and were thus more stable, which was also observed in the simulation results of the amplifier.

The steady-state response of the amplifier output is shown in Figure 5.11. From this, it is clear that the output signal is not distorted since the amplifier is not driven close to its saturation point. There AC hum is also visible on the output of this power supply which has a very small effect on the output signal of the amplifier.
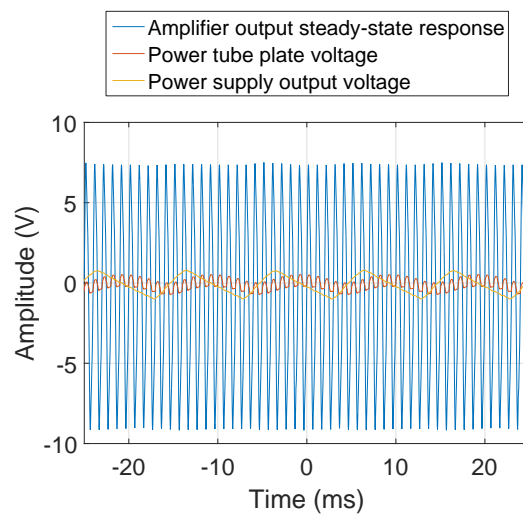
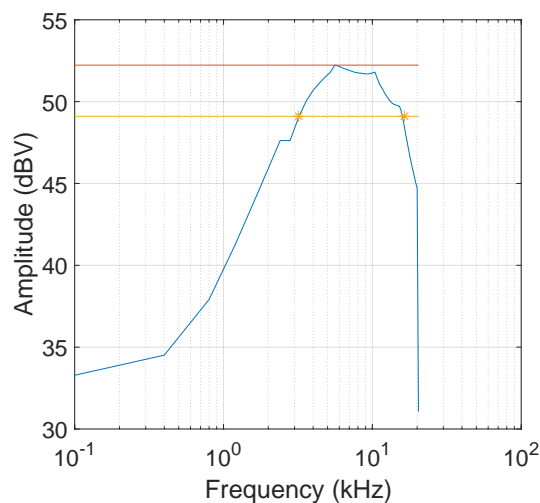**Figure 5.11.** Fender Deluxe 5E3 steady-state response when powered by the unregulated power supply.

Figure 5.12. Fender Deluxe 5E3 output frequency response when powered by the unregulated power supply.

The frequency response of the amplifier is shown in Figure 5.12. From this, it can be concluded that the Fender Deluxe 5E3 amplifier has a bandwidth of 15.4 kHz. These results confirm that the bandwidth of the amplifier is within the human audible range and that the amplifier will act as a low pass filter.

The output distortion of the Fender Deluxe 5E3 can be seen in Figure 5.13. This figure compares the sinusoidal input signal of 1 kHz of the amplifier to the output signal to determine the THD at high
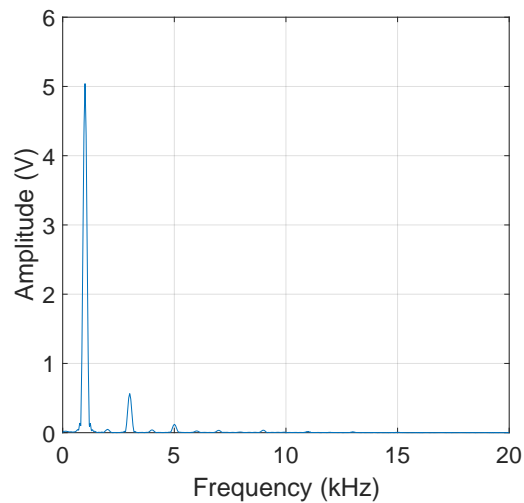
Figure 5.13. Fender Deluxe 5E3 output distortion of a 1 kHz sine wave.

volume levels. The THD is calculated as 11.11%

5.4.2   Measurements with the switch-mode power supply

The switch-mode power supply was constructed and tested to obtain data to compare to the amplifier measurements while it was powered by the unregulated power supply. This was done to confirm that the switch-mode power supply is accurate. The measurements in Table 5.3 were taken to ensure that the power supply voltages and bias voltages could be compared to the measurements of the amplifier while being powered by the unregulated power supply. From these results, it was confirmed the designed switch-mode power supply does generate the necessary output voltages required by the amplifier to function correctly.

The AC component of the output steady-state response results of the Fender Deluxe 5E3 switch-mode power supply section are shown in Figure 5.14 and the steady-state output response which shows the switching noise is shown in Figure 5.15. The gradient on the signal of the output of the amplifier in Figure 5.15 is due to the AC hum present on the output of the amplifier. The transient response of the switch-mode power supply is shown in Figure 5.16. From these graphs, it is clear that the power supply output is not regulated very strictly since the output of the high voltage supply drop when a load is suddenly connected and then recovers with some overshoot when the load is disconnected. It can be seen that the switch-mode controller attempt to regulate the output of the power supply but fails

Table 5.3. Voltage measurements of the amplifier when powered by the switch-mode power supply.

Parameter	Value
High voltage on the output transformer	428.2 V
Plate voltage on output tube 1	419.1 V
Plate voltage on output tube 2	419.4 V
High voltage for output tube screens	385.6 V
High voltage for pre-amplifier tube plates	277.3 V
Voltage over output tube biasing resistor	27.9 V
Voltage over 12AY7 tube biasing resistor	2.25 V
Voltage over 12AX7 tube biasing resistor	1.41 V
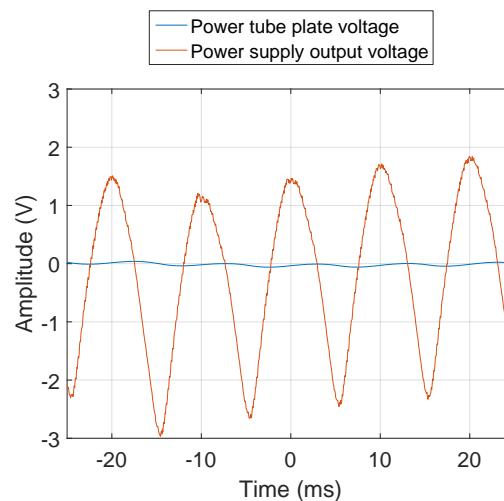
Figure 5.14. Fender Deluxe 5E3 switch-mode power supply steady-state response.

to do so when the current demand is too high. Once the current demand return to normal the controller manages to regulate the output of the power supply as can be seen by the overshoot. The high voltage supplied to the power amplifier and pre-amplifier stages had less output voltage ripple and were thus more stable, which was also observed in the simulation results of the amplifier.

The steady-state response of the amplifier is shown in Figure 5.17. It is evident that the output signal is not distorted since the amplifier is not driven close to its saturation point. This graph compares well to that in Figure 5.11 when the amplifier was powered by the unregulated power supply. There is also
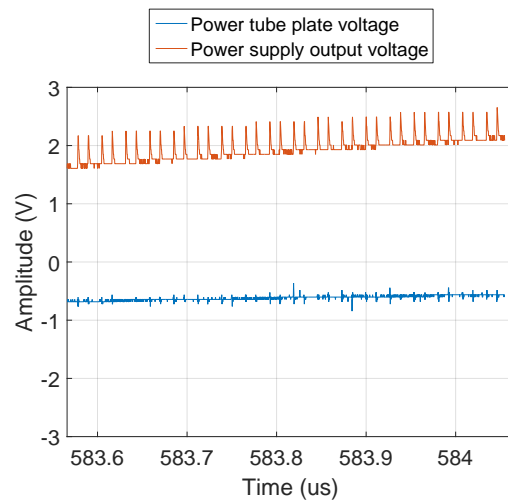
Figure 5.15. Fender Deluxe 5E3 switch-mode power supply steady-state response with switching noise.
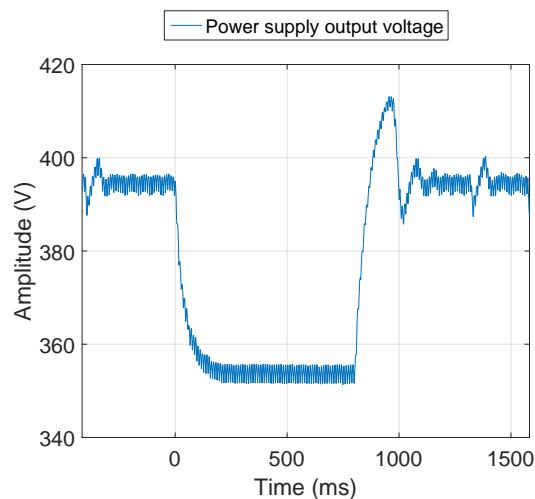

Figure 5.16. Fender Deluxe 5E3 switch-mode power supply transient response.

some AC hum visible on the output of the power supply.

The frequency response of the amplifier is shown in Figure 5.18. From this, it is evident that the Fender Deluxe 5E3 amplifier has a bandwidth of 15.4 kHz and confirmed that the bandwidth is the same as when it was powered by the unregulated power supply.

The output distortion of the Fender Deluxe 5E3 can be seen in Figure 5.19. This figure compares the
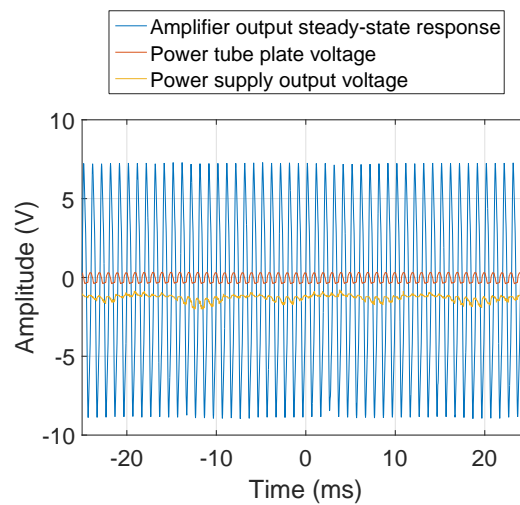
Figure 5.17. Fender Deluxe 5E3 steady-state response when powered by the switch-mode power supply.

Table 5.4. Speaker electrical parameter measurements.

Parameter	Value
DC resistance	6.92 Ω
Inductance	0.72 mH

sinusoidal input signal of 1 kHz of the amplifier to the output signal to determine the THD at high volume levels. The THD is calculated as 11.36%. This distortion level compares well to that of the amplifier when it was powered by the unregulated power supply and confirms that the same level of distortion could be obtained from the amplifier when it was powered by the switch-mode power supply.

5.5   SPEAKER CABINET PRACTICAL MEASUREMENTS

Measurements of the speaker cabinet with two parallel connected speakers are shown in Table 5.4. These values were compared to that of the speaker model that was developed to ensure that it was accurate.
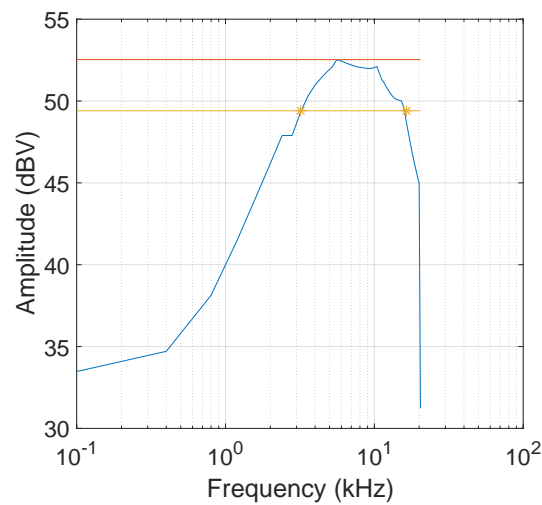
Figure 5.18. Fender Deluxe 5E3 output frequency response when powered by the switch-mode power supply.
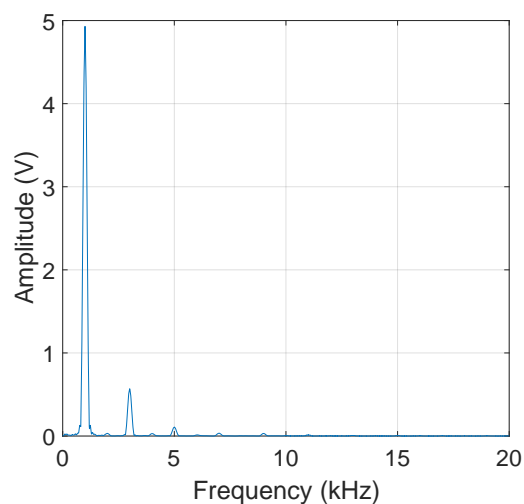
Figure 5.19. Fender Deluxe 5E3 output distortion of a 1 kHz sine wave.

The output transient response of the amplifier with the speaker cabinet connected is shown in Figure 5.20. Measurements were taken at several volume levels to compare to that of the amplifier with the speaker model connected.

The frequency response of the amplifier with the speaker connected is shown in Figure 5.21. The amplifier was tested over a frequency range of 1 Hz to 20 kHz for the selected volume setting.
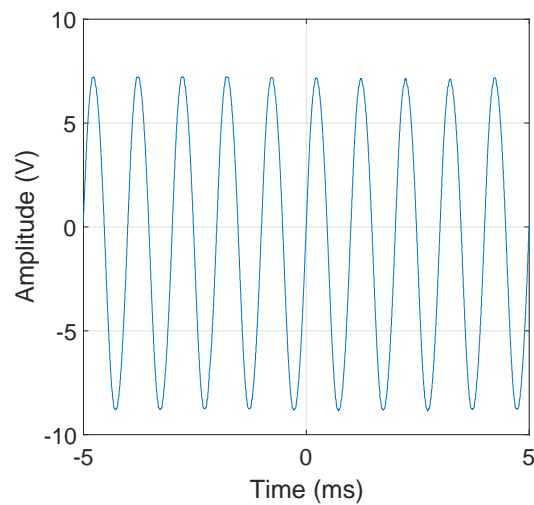
Figure 5.20. Fender Deluxe 5E3 transient response with the speaker connected.
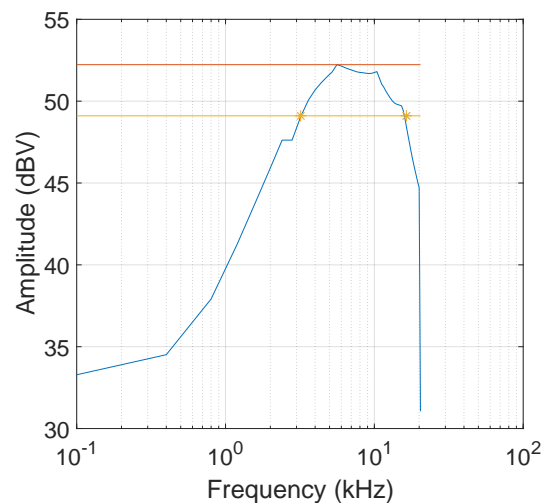
Figure 5.21. Fender Deluxe 5E3 output frequency response with the speaker connected.

The output distortion of the amplifier with the speaker cabinet connected is illustrated in Figure 5.22. This figure compares the sinusoidal input signal of 1 kHz of the amplifier to the output signal to determine the THD at high volume levels. The THD is calculated as 2.18%.

5.6   SPEAKER MODEL PRACTICAL MEASUREMENTS

Measurements of the speaker model with two parallel connected speakers are shown below in Table 5.5. These values were compared to that of the speaker cabinet to ensure that the model met the design

Figure 5.22. Fender Deluxe 5E3 output distortion of a 1 kHz sine wave with the speaker cabinet.

Table 5.5. Speaker model electrical parameter measurements.

Parameter	Value
DC resistance	6.98 Ω
Inductance	0.51 mH

requirements and that it could be used to test the amplifier.

The output transient response of the amplifier with the speaker model connected is shown in Figure 5.23. Measurements were taken at several volume levels to compare to that of the amplifier with the speaker cabinet connected. This transient response compares well to that of the speaker cabinet.

The frequency response of the amplifier with the speaker model connected is shown in Figure 5.24. The amplifier was tested over a frequency range of 1 Hz to 20 kHz for the selected volume setting. It was done to confirm that the bandwidth of the amplifier does not change. Comparing this result to that of the speaker cabinet, it is evident that both the speaker cabinet and speaker model have the same bandwidth.

The output distortion of the amplifier with the speaker model connected is found in Figure 5.25. This figure compares the sinusoidal input signal of 1 kHz of the amplifier to the output signal to determine the THD at high volume levels. The THD is calculated as 11.11%.

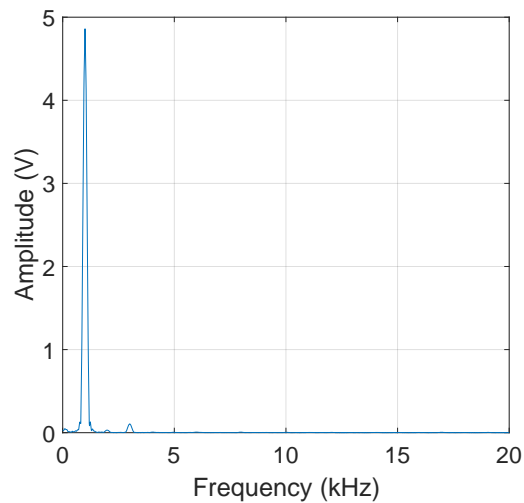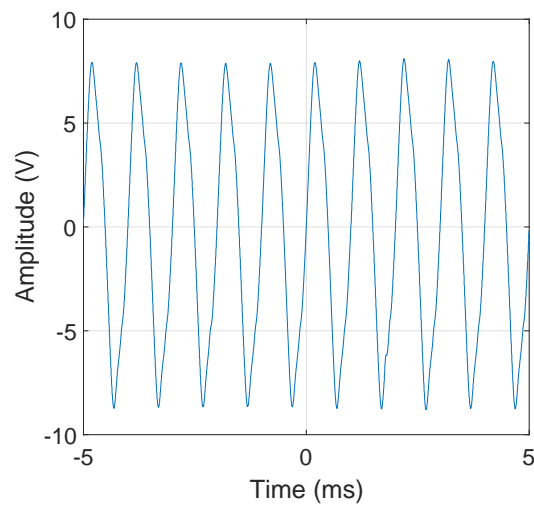**Figure 5.23.** Fender Deluxe 5E3 transient response with the speaker model connected.
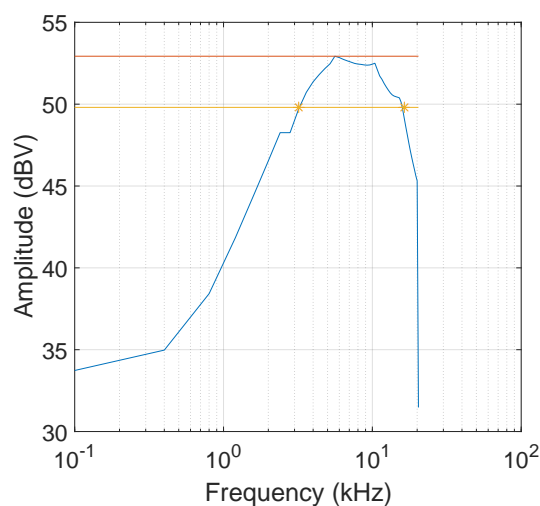
Figure 5.24. Fender Deluxe 5E3 output frequency response with the speaker model connected.

5.7   CHAPTER CONCLUSION

This chapter presented the simulation model that was used to simulate the amplifier in order to test different power supply designs on the amplifier. Measurement results of the simulation model, the amplifier while being powered by the unregulated power supply with valve rectifiers, and the amplifier while being powered by the switch-mode power supply was given. These results were also discussed individually. Measurement results of the speaker cabinet model were also given to show that the speaker model was accurate and could thus be used to replace the speaker in most of the tests.

Figure 5.25. Fender Deluxe 5E3 output distortion of a 1 kHz sine wave with the speaker cabinet.

CHAPTER 6   DISCUSSION

6.1   CHAPTER OVERVIEW

The results from the measurements when the amplifier was powered by the unregulated and switch-mode power supply, respectively, are discussed in this section. The measurements of the speaker cabinet and speaker model are also discussed to determine if the speaker model could be used to test the amplifier without changing the output response.

6.2   FENDER DELUXE 5E3 MEASUREMENT DISCUSSION

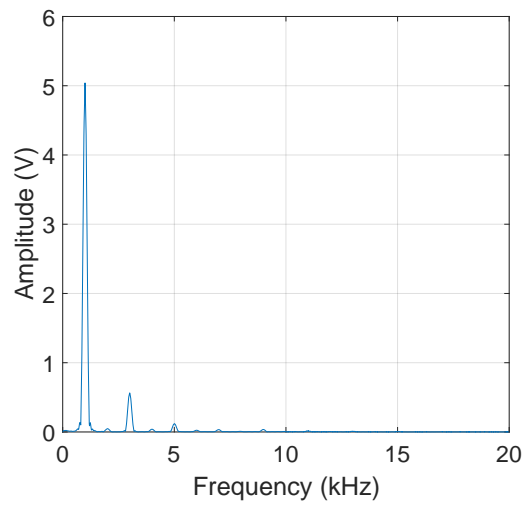The Fender Deluxe 5E3 amplifier was chosen to perform this study since this amplifier is a relatively simple amplifier to construct and it has a push-pull configuration which is also used in larger amplifiers. This amplifier also has a relatively low output power so it is possible to drive the amplifier into saturation in a residential area without creating a disturbance and the Fender Deluxe 5E3 is also a well-known design.

The power supply voltages of the amplifier simulation model, of the amplifier, powered by the unregulated power supply, and of the amplifier powered by the switch-mode power supply, shown in Tables 5.1 to 5.3 respectively, are similar and thus implies that the power supply section of the simulation model is accurate and that the output voltage of the switch-mode power supply is within the designed limits.

The output impedance of the unregulated power supply is a bit higher than that of the switch mode power supply. This can mostly be attributed to the smaller inductance and lower inductor resistance

of the switch-mode power supply, the dependency on the duty cycle and also to the much higher operating frequency of the switch-mode power supply. The impedance of the capacitors and inductors in the circuits are highly dependent on the frequency at which they operate. The output impedance of the switch-mode power supply is roughly the same over the whole operating frequency range while the unregulated power supply has a fixed output impedance due to the fixed 50 Hz AC input that it receives.

The steady-state response of the amplifier simulation model, shown in Figure 5.6, compares well to that of the steady-state response of the amplifier powered by the unregulated power supply, shown in Figure 5.11, and to that of the amplifier powered by the switch-mode power supply, shown in Figure 5.17. The transient response of the power supply in the amplifier simulation model, shown in Figure 5.5, compares well to the transient response of the unregulated power supply in the amplifier, shown in Figure 5.10, and to the switch-mode power supply in the amplifier, shown in Figure 5.16. The transient response of the switch-mode power supply does not have any 50 Hz hum present on the output and also have some overshoot when the test load is removed. This should, however, not affect the sound of the amplifier except for the fact that the amplifier will not have any 50 Hz hum present on its output. It can be seen that there is AC hum present on all three of the outputs of the respective power supplies. The switching noise can also be seen in Figure 5.15, which is much higher than the high cut off frequencies for the amplifier and speaker system, implying that the switching noise is not present on the audio signal of the amplifier. This implies that the switch-mode power supply is accurate in terms of the output transient response since this response and that of the amplifier powered by the switch-mode power supply is similar.

The frequency response of the simulation model, shown in Figure 5.8, is similar to that of the amplifier powered by the unregulated power supply, shown in Figure 5.13, and that of the amplifier powered by the switch-mode power supply, shown in Figure 5.19. The output distortion of the amplifier when powered by the unregulated and switch-mode power supply, respectively, is shown in Figure 6.1. This implies that the switch-mode power supply did not add any additional switching noise within the human audible range compared to when the amplifier was powered by the unregulated power supply. This also shows that the level of distortion produced by the amplifier did not change when it was powered by the switch-mode power supply.

From these comparisons, it can be concluded that the switch-mode power supply was accurate enough
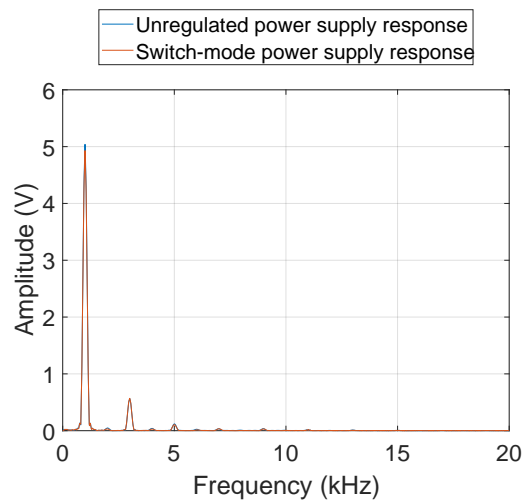
Figure 6.1. Fender Deluxe 5E3 output distortion when powered by the unregulated and switch-mode power supply, respectively.

to simulate the unregulated power supply of the amplifier. It was thus unnecessary to test the sound with a calibrated microphone since the measurement of the amplifier output, while it was connected to the speaker, will give similar or worse results. This can be justified by taking a look at the frequency response of the speaker and noting that it has a sharp drop-off on the frequency response after 20 kHz, which falls outside the human audible range. This means that all of the switching noise above 20 kHz were suppressed even further by the speaker. The design of the frequency clamped critical conduction mode boost converter ensured that the switching frequency was high enough. The frequency of the boost converter is clamped between 55 kHz and 80 kHz. By comparison, subjective tests would have been difficult to control in order to ensure that repeatable results are obtained. For example, the experience of the person and the room that the speaker is placed in can influence the result.

The motivation for choosing the non-isolated boost converter topology was that this topology is compact and fairly effective. This converter can supply voltages that are high enough to power the valve amplifier and isolation can easily be obtained by using a small forward or flyback converter in front of the boost converter and by removing the rectifying circuitry from the boost converter. The isolation circuitry was not included in the design since this will not have any effect on the valve amplifier. An isolation transformer was used to isolate the switch-mode power supply from the mains supply in order to safely test the switch-mode power supply.

6.3   SPEAKER AND SPEAKER MODEL MEASUREMENTS DISCUSSION

The transient response of the amplifier with either the speaker cabinet or the speaker model connected are shown in Figure 6.2 to compare the respective output responses. The frequency response of the amplifier with the speaker cabinet and that of the amplifier with the speaker model at a frequency of 1 kHz is shown in Figure 6.3. From these figures, it can be concluded that the performance of the speaker model is similar to that of the speaker over a volume range of 4 to 8. The volume range of 4 to 8 stretches from minimal to significant signal distortion to ensure that the whole range of the amplifier, as well as the speaker model, was tested. This implies that the simulation model is valid for the same volume range and that it could be used in simulations to test the amplifier.

The difference in performance on a volume setting of 2 can be contributed to the fact that the speaker model incorporates the acoustical as well as the mechanical characteristics of the speaker over the entire volume range. These characteristics will differ from that of the speaker on low volume settings because the speaker cone does not move as vigorously on low volumes as on higher volume settings.

Figure 6.3 shows that the distortion measurement is higher on the speaker model when compared to the distortion of the speaker cabinet. This is however not a problem since the amplifier will have the same amount of distortion whether the amplifier is powered by the unregulated or switch-mode power supplies. It should, however, be noted that the amplifier will have a lower total harmonic distortion when it is tested with the speaker connected, but this will not influence the outcome of this study since the speaker model was used for all of the tests that were performed with the different power supplies.

6.4   CHAPTER CONCLUSION

The results from Chapter 5 were discussed in detail in this chapter. This was done to determine that it was possible to replace the unregulated power supply using valve rectifiers with a switch-mode power supply without affecting the sound and performance of the amplifier. The results from the amplifier when either the speaker or speaker model were connected were also discussed to conclude that the tests that were performed on the amplifier with the speaker model connected were relevant and accurate.

(a) Volume level 2.

(b) Volume level 4.

(c) Volume level 6.
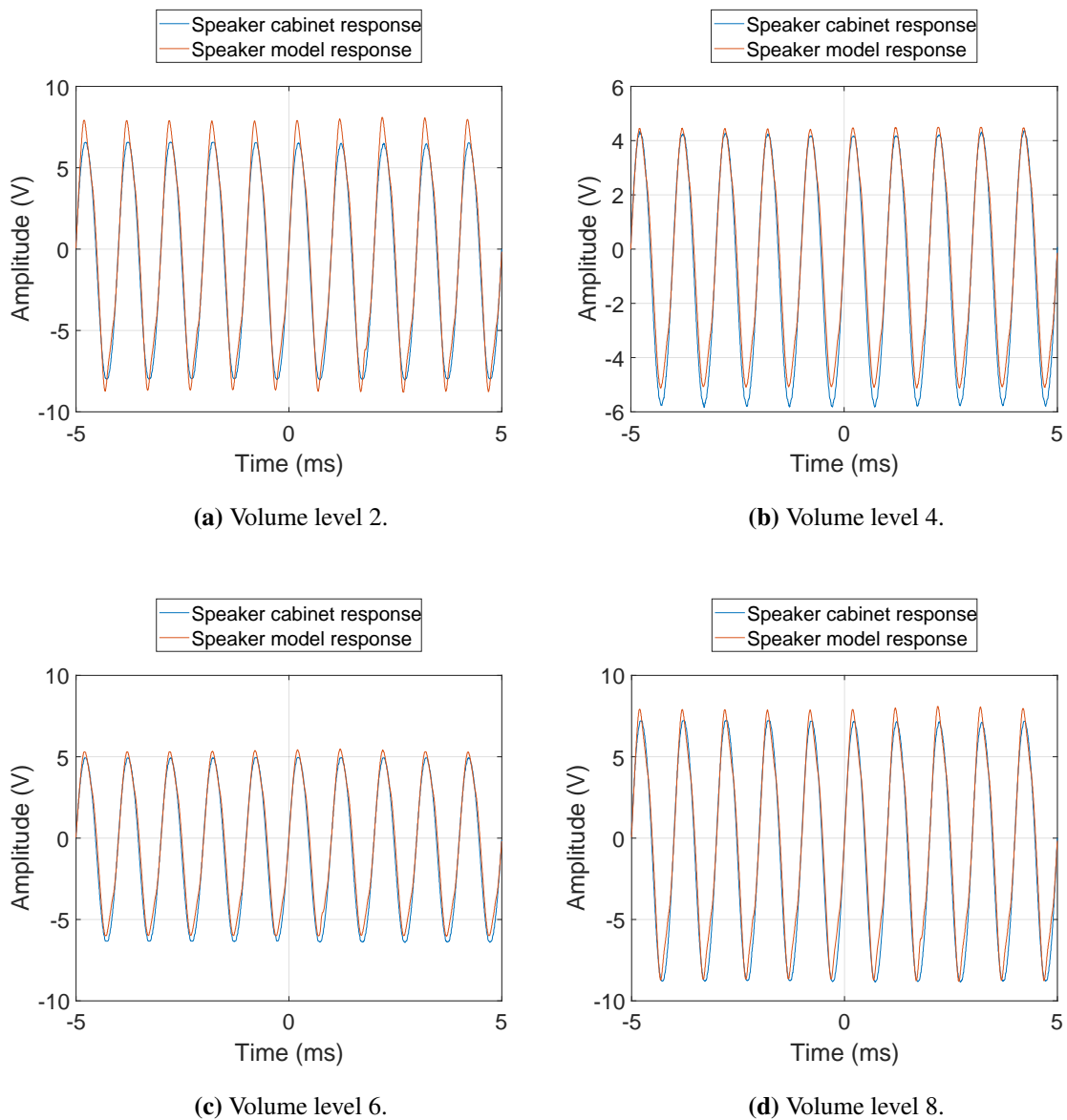
(d) Volume level 8.

Figure 6.2. Speaker and speaker model transient response comparison with different volume levels.

(a) Volume level 2.

(b) Volume level 4.

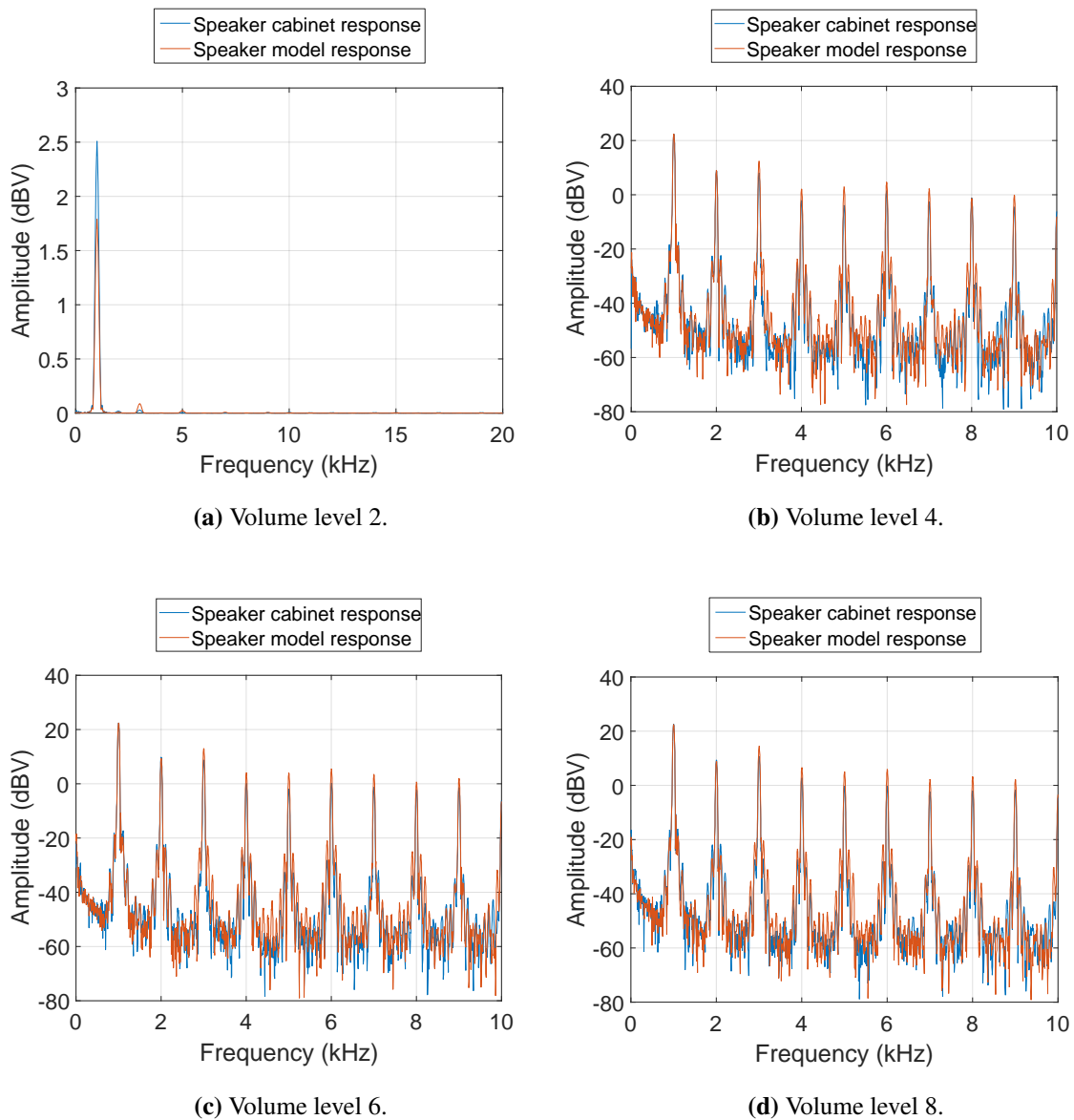**(c)** Volume level 6.

(d) Volume level 8.

Figure 6.3. Speaker and speaker model frequency response comparison with different volume levels at 1 kHz.

CHAPTER 7   CONCLUSION

The goal of this research was to select a switch-mode power supply topology that would be able to replace an unregulated power supply using valve rectifiers in a valve amplifier with the same output response as that of the commonly used unregulated valve power supply. One topology was selected and analysed to understand which parts of the circuit were responsible for the transient and frequency responses and how to change these responses to obtain the desired result. The desired response had to be obtained from the switch-mode power supply while still maintaining a rough level of output regulation. This ensured that the power supply did not go into an under or over voltage situation where it would be shut down by the protection circuitry.

From the analyses done in this project, it is clear that the transient response of the switch-mode power supply can be slightly changed in the circuit by changing the output bulk capacitors and current limiting resistors, or voltage drop resistors, especially with regard to the amount of output voltage ripple. It is, however, also clear that most of the transient response was obtained from a sluggish feedback loop which allowed the output voltage to sag and then to steadily recover. The controller in the switch-mode power supply was used to change the transient response by limiting the output current to ensure that the output started to sag and that voltage ripple was present on the output when the amplifier was driven into saturation when the guitar was being played forcefully.

The research confirmed that the frequency response of the switch-mode power supply can be changed by manipulating the output circuitry. This was accomplished by designing a low pass output filter that has a cut-off frequency which is just outside the human audible range. The use of a frequency clamped critical conduction mode boost converter also ensured that the switching frequency was well above the human audible range. This ensured that switching noise from the boost converter was not present in the working frequency range of the amplifier.

The use of a speaker cabinet model made it possible to test the amplifier inside residential areas on high volumes without causing a disturbance. It was unnecessary to test the amplifier with a microphone and audio analyses since the output of the amplifier could easily be measured using an oscilloscope. This allowed for accurate and repeatable measurements that could be compared to each other when the amplifier was powered from the switch-mode or unregulated power supply, respectively. It also ensured that the worst case measurement could be taken since the speaker and cabinet suppressed any high-frequency switching noise even further because the speaker had the same frequency response as a band-pass filter.

It was found that fluctuations in the power supply voltage affected the output stage of the amplifier. This is because this stage of the amplifier draws the most current and the characteristic response of the power tube is affected by fluctuations in the supply or plate voltage. A drop in the plate voltage also causes a drop in the plate current. This, in turn, affects the bias current of the self-biasing circuit which will move the operating point on the characteristic curve of the vacuum tube. When the amplifier is near or in its saturation region, the power supply output voltage will continuously fluctuate which will cause the bias point to continuously move around. This constant moving bias point produces a unique sound that solid-state amplifier designers still have trouble with to replicate.

The power supply has an influence on the dynamic response of a valve amplifier. The amount of clipping in the power stage of the amplifier is dependent on the output voltage of the power supply. The output voltage and the output impedance also have an influence on the characteristic curve of the vacuum tube and, therefore, on the sound of the amplifier. The power supply could thus be used to move the operating point on the characteristic curve of the vacuum tube.

It was possible to recreate the power supply saturation response of an unregulated linear power supply with a carefully designed switch-mode power supply. This was achieved by modifying the feedback network to obtain a slower output response.

From the research, it can be concluded that it is indeed possible to power a high power valve amplifier with a switch-mode power supply that delivers an unregulated response. It was found that the sound of the amplifier was not affected by the new power supply and that no switching noise was added to the output. The results obtained from this study will enable designers to design smaller and lighter in weight valve amplifiers which can be transported more easily.

7.1 FUTURE RESEARCH

For future research, a higher power class AB amplifier can be used to perform the measurements to ensure that the results are still valid if the output power of the amplifier is increased. Different switch-mode power supply topologies can be tested to obtain a switch-mode power supply that provides isolation from the mains AC voltage without using a dedicated isolation transformer.

The speaker model can also be developed further to allow longer testing at high output volumes without the model heating up and becoming inaccurate. This will allow testing of the amplifiers for prolonged periods at high output volumes to study the effects that heat has on the output tubes and ultimately on the sound produced by the amplifier.

A system which is capable of automatically biasing the output valves individually can also be developed which would be extremely beneficial. This will remove the need for musicians to send their amplifiers to a technician to bias the output valves, which can be a tedious and time-consuming task.

REFERENCES

[1] H. Peavey, "Standby... For the Truth," Peavey Electronics corporation Whitepapers, Mississippi, United States, Tech. Rep., 2006.

[2] B. Brusso and B. Bose, "Power electronics Historical perspective and my experience [history]," *IEEE Industry Applications Magazine*, vol. 20, no. 2, pp. 7–81, Mar. 2014.

[3] J. Werner, S. V. G. Oliveira, and A. Péres, "Design and implementation of a DC-DC flyback converter to feed a class a tube amplifier," in *COBEP 2011 – 11th Brazilian Power Electronics Conference*. IEEE, Sep. 2011, pp. 992–996.

[4] E. Barbour, "Cool sound of tubes," *IEEE Spectrum*, vol. 35, no. 8, pp. 24–35, 1998.

[5] H. Peavey, "How All This Came About," Peavey Electronics corporation Whitepapers, Mississippi, United States, Tech. Rep., 2006.

[6] M. Jones, *Valve amplifiers*, 3rd ed. United States: Oxford, 2003.

[7] D. Self, *Audio Power Amplifier Design Handbook*, 3rd ed. United States: Newnes, 2002.

[8] L. M. Vallese, "Upper limits of output power in vacuum-tube and transistor A-C amplifiers," *Transactions of the American Institute of Electrical Engineers, Part I: Communication and Electronics*, vol. 76, no. 1, pp. 87–92, 1957.

REFERENCES

[9] B. Bowers, "A century of electronics [the evolution of vacuum tubes]," *IEE Review*, vol. 50, no. 11, pp. 36–39, Nov. 2004.

[10] H. Peavey, "TransTube," Peavey Electronics corporation Whitepapers, Mississippi, United States, Tech. Rep. 6, 2006.

[11] A. J. Winter, "The effect of filament voltage upon vacuum tube characteristics," *Transactions of the IRE Professional Group on Electron Devices*, vol. PGED-2, no. 2, pp. 47–59, Jan. 1953.

[12] J. Wilson, "When hand-built is cooler [manufacturing retro audio]," *Engineering & Technology*, vol. 4, no. 18, pp. 60–62, 2009.

[13] S. A. Shirsavar, "Teaching practical design of switch-mode power supplies," *IEEE Transactions on Education*, vol. 47, no. 4, pp. 467–473, Nov. 2004.

[14] J. J. Shieh, "Analysis and design of parallel-connected peak-current-mode-controlled switching DC/DC power supplies," *IEE Proceedings-Electric Power Applications*, vol. 151, no. 4, pp. 434–442, 2004.

[15] B. Allard, S. Trochut, X. Lin-Shi, and J.-M. Retif, "Control design for integrated switch-mode power supplies: a new challenge?" in *IEEE 35th Annual Power Electronics Specialists Conference*, vol. 6, 2004, pp. 4492–4497.

[16] G. Liebmann, "The Calculation of Amplifier Valve Characteristics," *Journal of the Institution of Electrical Engineers - Part III: Radio and Communication Engineering*, vol. 93, no. 23, pp. 138–152, 1945.

[17] Z. Sari and K. Amgoud, "Design and implementation of a microprocessor based high frequency switching mode power supply," *European Power Electronics Association*, no. 9, pp. 334–337, Sep. 1993.

[18] M. O. Popescu and B. M. Radomirescu, "Design of IC controlled switched-mode supply with power factor correction," in *Industrial Electronics, 1995. ISIE '95., Proceedings of the IEEE*

International Symposium on, vol. 1. IEEE, 1995, pp. 416–420.

[19] M. Kamil, "AN1114-Switch Mode Power Supply (SMPS) Topologies," Microchip, Tech. Rep. Part I & 2, 2007.

[20] A. A. A. Abdelrahman, E. E. O. Elfaki, and H. A. ElnazirAdam, "Design of high frequency transformer for switch mode power supply," *International Conference on Computing, Control, Networking, Electronics and Embedded Systems Engineering (ICCNEEE)*, pp. 129–135, Sep. 2015.

[21] Y. P. Chan, M. H. Pong, N. K. Poon, and C. P. Liu, "Effective switching mode power supplies common mode noise cancellation technique with zero equipotential transformer models," in *Conference Proceedings - IEEE Applied Power Electronics Conference and Exposition - APEC*. IEEE, Feb. 2010, pp. 571–574.

[22] M. R. Yazdani, H. Farzanehfard, and J. Faiz, "Conducted EMI modeling and reduction in a flyback switched mode power supply," in *2011 2nd Power Electronics, Drive Systems and Technologies Conference, PEDSTC 2011*. IEEE, Feb. 2011, pp. 620–624.

[23] L. Wuidart, "Topologies for switched mode power supplies," ST Microelectronics, Geneva, Switzerland, Tech. Rep., 1999.

[24] M. J. Humphreys, D. Brown, L. Burley, C. J. Hammerton, and R. Miller, "Switched Mode Power Supplies," Phillips, Tech. Rep., 2010.

[25] V. Skanda, "AN1106-Power Factor Correction in Power Conversion Applications Using the dsPIC DSC," Microchip, Tech. Rep. 1, 2007.

[26] N. E. Iversen, "Introduction to loudspeaker modelling & design," Technical University of Denmark, Tech. Rep., Sep. 2014.

ADDENDUM A   AMPLIFIER REFERENCE SCHEMATICS

A.1   FENDER DELUXE 5E3 SCHEMATIC

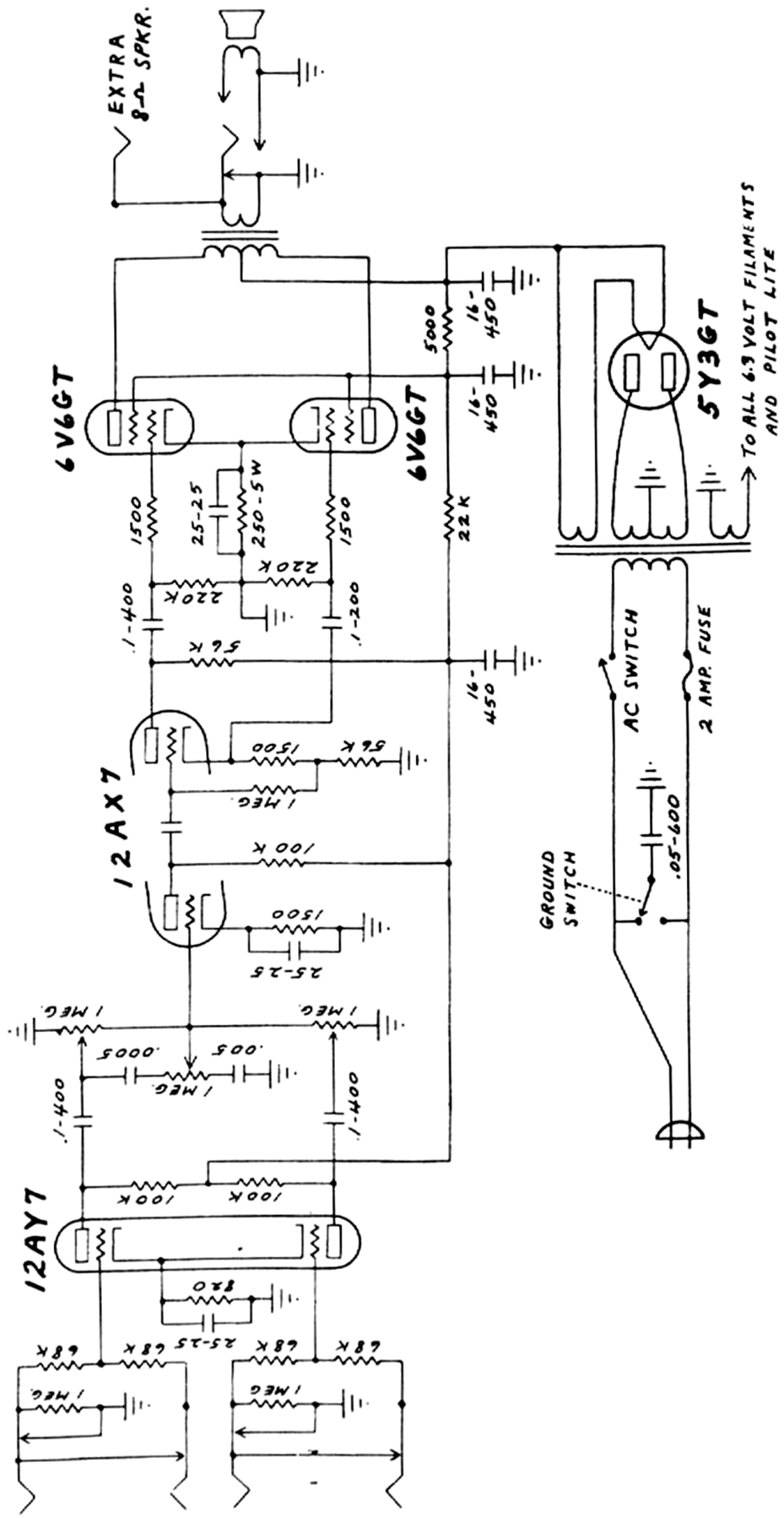**Figure A.1.** Fender Deluxe 5E3 schematic.

ADDENDUM B   TUBE MODEL PARAMETERS

B.1   TUBE DIODE MODEL PARAMETERS

B.1.1   5Y3GT diode model

```
*            Plate
*              |
*              | Cathode
*              | |
.SUBCKT 5Y3GT A K
GP  A   K   VALUE={2.69E-4*(PWR(V(A,K),1.5)+PWRS(V(A,K),1.5))/2}
.ENDS 5Y3GT
```

B.1.2   EZ81 diode model

```
*            Plate
*              |
*              | Cathode
*              | |
.SUBCKT EZ81 A K
BIA A K I=URAMP(V(A,K))**1.5 * 0.001677051
.ENDS
```

B.2 TRIODE MODELS

B.2.1 12AX7 model

```
* Generic triode model: 12AX7
* Copyright 2003--2008 by Ayumi Nakabayashi, All rights reserved.
* Version 3.10, Generated on Sat Mar  8 22:41:09 2008
*              Plate
*              | Grid
*              | | Cathode
*              | | |
.SUBCKT 12AX7 A G K
BGG   GG   0 V=V(G,K)+0.59836683
BM1   M1   0 V=(0.0017172334*(URAMP(V(A,K))+1e-10))**-0.2685074
BM2   M2   0 V=(0.84817287*(URAMP(V(GG)+URAMP(V(A,K))/88.413802+1e-10))
   **1.7685074
BP    P    0 V=0.001130216*(URAMP(V(GG)+URAMP(V(A,K))/104.24031)+1e-10)
   **1.5
BIK   IK   0 V=U(V(GG))*V(P)+(1-U(V(GG)))*0.00071211506*V(M1)*V(M2)
BIG   IG   0 V=0.000565108*URAMP(V(G,K))**1.5*(URAMP(V(G,K))/(URAMP(V(A,K
   ))+URAMP(V(G,K)))*1.2+ 0.4)
BIAK  A    K I=URAMP(V(IK,IG)-URAMP(V(IK,IG)-(0.00058141055*URAMP(V(A,K))
   **1.5)))+ 1e-10*V(A,K)
BIGK  G    K I=V(IG)
CGA   G    A 1.7p
CGK   G    K 1.6p
CAK   A    K 0.5p
.ENDS
```

B.2.2   12AY7 model

```
* Generic triode model: 12AY7
* Copyright 2003--2008 by Ayumi Nakabayashi, All rights reserved.
* Version 3.10, Generated on Sat Mar  8 22:41:10 2008
*           Plate
*           | Grid
*           | | Cathode
*           | | |
.SUBCKT 12AY7 A G K
BGG   GG   0 V=V(G,K)+0.71171435
BM1   M1   0 V=(0.0094119714*(URAMP(V(A,K))+1e-10))**-0.68363668
BM2   M2   0 V=(0.68692746*(URAMP(V(GG)+URAMP(V(A,K))/33.263227)+1e-10))
   **2.1836367
BP    P    0 V=0.00092634255*(URAMP(V(GG)+URAMP(V(A,K))/48.423202)+1e-10)
   **1.5
BIK   IK   0 V=U(V(GG))*V(P)+(1-U(V(GG)))*0.00054133951*V(M1)*V(M2)
BIG   IG   0 V=0.00046317128*URAMP(V(G,K))**1.5*(URAMP(V(G,K))/(URAMP(V(A
   ,K))+URAMP(V(G,K)))* 1.2+0.4)
BIAK  A    K I=URAMP(V(IK,IG)-URAMP(V(IK,IG)-(0.00049201413*URAMP(V(A,K))
   **1.5)))+         1e-10*V(A,K)
BIGK  G    K I=V(IG)
CGA   G    A 1.3p
CGK   G    K 1.3p
CAK   A    K 0.6p
.ENDS
```

B.3   PENTODE MODELS

B.3.1   EL84 model

```
* Generic pentode model: EL84_AN
* Copyright 2003--2008 by Ayumi Nakabayashi, All rights reserved.
* Version 3.10, Generated on Wed Feb 12 10:18:18 2014
*               Plate
*               | Screen Grid
*               | |  Control Grid
*               | |  |  Cathode
*               | |  |  |
.SUBCKT EL84_AN A G2 G1 K
BGG   GG   0 V=V(G1,K)+0.03372597
BM1   M1   0 V=(0.014266539*(URAMP(V(G2,K))+1e-10))**-0.43210132
BM2   M2   0 V=(0.7763568*(URAMP(V(GG)+URAMP(V(G2,K))/15.676066)))
   **1.9321013
BP    P    0 V=0.0040800354*(URAMP(V(GG)+URAMP(V(G2,K))/20.191832))**1.5
BIK   IK   0 V=U(V(GG))*V(P)+(1-U(V(GG)))*0.0023829269*V(M1)*V(M2)
BIG   IG   0 V=0.0020400177*URAMP(V(G1,K))**1.5*(URAMP(V(G1,K))/(URAMP(V(
   A,K))+URAMP(V(G1,K)))*1.2+0.4)
BIK2  IK2  0 V=V(IK,IG)*(1-0.4*(EXP(-URAMP(V(A,K))/URAMP(V(G2,K))*15)-EXP
   (-15)))
BIG2T IG2T 0 V=V(IK2)*(0.904015183*(1-URAMP(V(A,K))/(URAMP(V(A,K))+10))
   **1.5+0.095984817)
BIK3  IK3  0 V=V(IK2)*(URAMP(V(A,K))+2486)/(URAMP(V(G2,K))+2486)
BIK4  IK4  0 V=V(IK3)-URAMP(V(IK3)-(0.0023468355*(URAMP(V(A,K))+URAMP(
   URAMP(V(G2,K))-URAMP(V(A,K))))**1.5))
BIP   IP   0 V=URAMP(V(IK4,IG2T)-URAMP(V(IK4,IG2T)-(0.0023468355*URAMP(V(
   A,K))**1.5)))
BIAK  A    K I=V(IP)+1e-10*V(A,K)
BIG2  G2   K I=URAMP(V(IK4,IP))
BIGK  G1   K I=V(IG)
* CAPS
CGA   G1   A  0.5p
CGK   G1   K  6.6p
C12   G1   G2 4.4p
```

```
CAK    A   K   6.5p
.ENDS
```

B.3.2   6V6GT model

```
* Generic pentode model: 6V6
* Copyright 2003--2008 by Ayumi Nakabayashi, All rights reserved.
* Version 3.10, Generated on Sat Mar  8 22:41:04 2008
*          Plate
*          | Screen Grid
*          | |  Control Grid
*          | |  | Cathode
*          | |  | |
.SUBCKT 6V6 A G2 G1 K
BGG    GG   0 V=V(G1,K)+0.99999998
BM1    M1   0 BM1   M1   0 V=(0.048335289*(URAMP(V(G2,K))+1e-10))
   **-0.77023894
BM2    M2   0 V=(0.6607234*(URAMP(V(GG)+URAMP(V(G2,K))/7.0192317)))
   **2.2702389
BP     P    0 V=0.0010053341*(URAMP(V(GG)+URAMP(V(G2,K))/10.623555))**1.5
BIK    IK   0 V=U(V(GG))*V(P)+(1-U(V(GG)))*0.00060166202*V(M1)*V(M2)
BIG    IG   0 V=0.00051429562*URAMP(V(G1,K))**1.5*(URAMP(V(G1,K))/(URAMP(V
   (A,K))+URAMP(V(G1,K)))  *1.2+0.4)
BIK2   IK2  0 V=V(IK,IG)*(1-0.4*(EXP(-URAMP(V(A,K))/URAMP(V(G2,K))*15)-EXP
   (-15)))
BIG2T  IG2T 0 V=V(IK2)*(0.916000233*(1-URAMP(V(A,K))/(URAMP(V(A,K))+10))
   **1.5+ 0.083999767)
BIK3   IK3  0 V=V(IK2)*(URAMP(V(A,K))+3125)/(URAMP(V(G2,K))+3125)
BIK4   IK4  0 V=V(IK3)-URAMP(V(IK3)-(0.00061491868*(URAMP(V(A,K))+ URAMP(
   URAMP(V(G2,K))-URAMP(V(A,K))))**1.5))
BIP    IP   0 V=URAMP(V(IK4,IG2T)-URAMP(V(IK4,IG2T)-(0.00061491868*URAMP(V
   (A,K))**1.5)))
BIAK   A    K I=V(IP)+1e-10*V(A,K)
BIG2   G2   K I=URAMP(V(IK4,IP))
BIGK   G1   K I=V(IG)
CGA    G1   A  0.7p
CGK    G1   K  5p
```

```
C12   G1  G2 3.3p
CAK   A   K  6.9p
.ENDS
```